



HAL
open science

Paneth cell defects induce microbiota dysbiosis In mice and promote visceral hypersensitivity

Ambre Riba, Maïwenn Olier, Sonia Lacroix-Lamandé, Corinne Lencina, Valérie Alquier-Bacquié, Cherryl Harkat, Marion Gillet, Marine Baron, Caroline Sommer, Virginie Mallet, et al.

► To cite this version:

Ambre Riba, Maïwenn Olier, Sonia Lacroix-Lamandé, Corinne Lencina, Valérie Alquier-Bacquié, et al.. Paneth cell defects induce microbiota dysbiosis In mice and promote visceral hypersensitivity. *Gastroenterology*, 2017, 153, pp.1594-1606. 10.1053/j.gastro.2017.08.044 . hal-01603303

HAL Id: hal-01603303

<https://hal.science/hal-01603303>

Submitted on 26 May 2020

HAL is a multi-disciplinary open access archive for the deposit and dissemination of scientific research documents, whether they are published or not. The documents may come from teaching and research institutions in France or abroad, or from public or private research centers.

L'archive ouverte pluridisciplinaire **HAL**, est destinée au dépôt et à la diffusion de documents scientifiques de niveau recherche, publiés ou non, émanant des établissements d'enseignement et de recherche français ou étrangers, des laboratoires publics ou privés.

Accepted Manuscript

Paneth Cell Defects Induce Microbiota Dysbiosis In Mice And Promote Visceral Hypersensitivity

Ambre Riba, Maïwenn Olier, Sonia Lacroix-Lamandé, Corinne Lencina, Valérie Bacquié, Cheryl Harkat, Marion Gillet, Marine Baron, Caroline Sommer, Virginie Mallet, Christel Salvador-Cartier, Fabrice Laurent, Vassilia Théodorou, Sandrine Ménard

PII: S0016-5085(17)36077-8
DOI: [10.1053/j.gastro.2017.08.044](https://doi.org/10.1053/j.gastro.2017.08.044)
Reference: YGAST 61390

To appear in: *Gastroenterology*
Accepted Date: 24 August 2017

Please cite this article as: Riba A, Olier M, Lacroix-Lamandé S, Lencina C, Bacquié V, Harkat C, Gillet M, Baron M, Sommer C, Mallet V, Salvador-Cartier C, Laurent F, Théodorou V, Ménard S, Paneth Cell Defects Induce Microbiota Dysbiosis In Mice And Promote Visceral Hypersensitivity, *Gastroenterology* (2017), doi: 10.1053/j.gastro.2017.08.044.

This is a PDF file of an unedited manuscript that has been accepted for publication. As a service to our customers we are providing this early version of the manuscript. The manuscript will undergo copyediting, typesetting, and review of the resulting proof before it is published in its final form. Please note that during the production process errors may be discovered which could affect the content, and all legal disclaimers that apply to the journal pertain.



Comment citer ce document :

Riba, A., Olier, M., Lacroix Lamandé, S., Lencina, C., Bacquié, V., Harkat, C., Gillet, M., Baron, M., Sommer, C., Mallet, V., Salvador Cartier, C., Laurent, F., Théodorou, V., Ménard, S. (2017). Paneth cell defects induce microbiota dysbiosis In mice and promote visceral hypersensitivity. *Gastroenterology*, 153 (6), 1594-1606. DOI : 10.1053/j.gastro.2017.08.044

PANETH CELL DEFECTS INDUCE MICROBIOTA DYSBIOSIS IN MICE AND PROMOTE VISCERAL HYPERSENSITIVITY

Short title: Role of Paneth cells in visceral hypersensitivity

Ambre Riba¹, Maïwenn Olier¹, Sonia Lacroix-Lamandé², Corinne Lencina¹, Valérie Bacquié¹, Cherryl Harkat¹, Marion Gillet¹, Marine Baron¹, Caroline Sommer¹, Virginie Mallet¹, Christel Salvador-Cartier¹, Fabrice Laurent², Vassilia Théodorou¹, Sandrine Ménard¹.

¹ INRA, ToxAlim (Research Centre in Food Toxicology), team Neuro-Gastroenterology and Nutrition, Université de Toulouse, INRA, ENVT, INP-Purpan, UPS, Toulouse, France

² Equipe Apicomplexes et Immunité Mucosale (AIM), UMR 1282 INRA/Université-Infectiologie et Santé Publique (ISP), Centre INRA Val de Loire, Nouzilly, FRANCE

Abbreviations: AMA, antimicrobial activity; AMP, antimicrobial peptides; CD, Crohn's Disease; CFU, Colony Forming Unit; EMG, Electromyograph; GVHD, Graft-versus-host disease; GULDA, Gut Low-Density Array; IBD, Inflammatory Bowel Disease; IBS, Irritable Bowel Syndrome; MS, Maternal Separation; NEC, Necrotizing enterocolitis; PC, Paneth cells; PLS-DA, Partial least-squares discriminant analysis; TNF α , Tumor Necrosis Factor α ; VIP, Variable Importance in Projection.

Correspondence: Sandrine Ménard, INRA, ToxAlim (Research Centre in Food Toxicology), team Neuro-Gastroenterology and Nutrition, Université de Toulouse, INRA, ENVT, INP-

Purpan, UPS, 180 Chemin de Tournefeuille, 31027 Toulouse, France ;
sandrine.menard@inra.fr; Phone : + 33 5 82 06 64 08 ; Fax: + 33 5 61 28 51 45

Disclosures: The authors disclose no conflicts

Authors contributions: Conceived and designed the experiments: SM AR VT. Performed the experiments: AR MO SLL VB CH MG MB CS VM CSC SM. Analyzed the data: AR MO VT SM. SM wrote the manuscript, with AR, VT, MO, SLL and FL providing critical output.

Acknowledgments: The authors gratefully acknowledge Yannick Lippi and Claire Naylies from Transcriptomic impact of Xenobiotics platform for technical assistance for microbiota analysis.

ABSTRACT

Background & Aims: Separation of newborn rats from their mothers induces visceral hypersensitivity and impaired epithelial secretory cell lineages when they are adults. Little is known about the mechanisms by which maternal separation causes visceral hypersensitivity or its relationship with defects in epithelial secretory cell lineages.

Methods: We performed studies with C3H/HeN mice separated from their mothers as newborns and mice genetically engineered (Sox9^{flox/flox}-vil-cre on C57BL/6 background) to have deficiencies in Paneth cells. Paneth cells deficiency was assessed by lysozyme staining of ileum tissues and lysozyme activity in fecal samples. When mice were 50 days old, their abdominal response to colorectal distension was assessed by electromyography. Fecal samples were collected and microbiota were analyzed using GULDA quantitative PCR.

Results: Mice with maternal separation developed visceral hypersensitivity and defects in Paneth cells, as reported from rats, compared to mice without maternal separation. Sox9^{flox/flox}-vil-Cre mice also had increased visceral hypersensitivity compared to control littermate Sox9^{flox/flox} mice. Fecal samples from mice with maternal separation and from Sox9^{flox/flox}-vil-cre mice had evidence for intestinal dysbiosis of the microbiota, characterized by expansion of *Escherichia coli*. Daily gavage of conventional C3H/HeN adult mice with 10⁹ commensal *E. coli* induced visceral hypersensitivity. Conversely, daily oral administration of lysozyme prevented expansion of *E. coli* during maternal separation and visceral hypersensitivity.

Conclusions: Mice with defects in Paneth cells (induced by maternal separation or genetically engineered) have intestinal expansion of *E. coli* leading to visceral hypersensitivity. These findings provide evidence that Paneth cell function and intestinal dysbiosis are involved in visceral sensitivity.

Keywords: Stress, antimicrobial activity, abdominal pain, lysozyme.

INTRODUCTION

The intestine is colonized by trillions of commensal microorganisms that constitute a complex microbial community¹⁻³. These microorganisms live in symbiotic and mutualistic relationship with the host and, as such, the microbiota is essential for mediating physiology, metabolism and host immune response. Intestinal homeostasis relies on a tightly regulated crosstalk between commensal bacteria, intestinal epithelial cells and mucosal immune cells. Innate immunity provides the first line of defense against invading microorganisms and confers protection by triggering inflammatory and antimicrobial responses.

Paneth cells producing enteric antimicrobial peptides are important players in small intestine innate immunity. Paneth cells located at the bottom of crypts produce and secrete various antimicrobial proteins or peptides (AMP) like lysozyme, phospholipase A2 (PLA2), Reg3 lectins and α -defensin named cryptdin in mice (for review⁴). Many studies performed in rodent models highlight Paneth cells contribution in establishment of an appropriate colonization with commensal microbiota⁵ and host protection from enteric pathogens^{6,7}. Studies show that both, gut microbiota profile⁸ and AMP repertoire^{8,9} are dependent on mouse strain suggesting the role of Paneth cell AMP in shaping intestinal microbiota. Even though some AMPs are dependent on microbiota colonization, Paneth cells derived AMPs such as cryptdin¹⁰ lysozyme and PLA2^{11,12} are expressed independently of microbiota colonization.

A defect in Paneth cell numbers and/or antimicrobial activity (functionality) has been incriminated in susceptibility to enteric infections as well as in multifactorial organic gastrointestinal disorders like necrotizing enterocolitis (NEC)¹³ and Crohn's diseases (CD)^{14,15} both characterized by intestinal microbiota dysbiosis. One hypothesis is that Paneth cell failure

triggers microbiota dysbiosis in favor of opportunistic bacteria that might trigger intestinal disorders in predisposed individuals.

Furthermore, it is well accepted that genetic and environmental factors contribute to the development of organic gastrointestinal disorders like CD^{16,17} but also functional ones like Irritable bowel syndrome (IBS). Despite high discrepancies concerning the severity of intestinal inflammation between CD and IBS some common pathophysiological features such as visceral hypersensitivity¹⁸ and microbiota dysbiosis¹⁹ have been reported. Interestingly, among environmental factors affecting the course of these diseases, early life adverse events play a crucial role^{20,21}. Indeed, maternal separation (MS) performed in rat decreases epithelial secretory cell lineages including Paneth cells²² and induces visceral hypersensitivity²³. However, a mechanistic link between Paneth cell defect and visceral hypersensitivity has never been investigated.

In the present study, by establishing a mouse model of MS and using various mouse models including Sox9^{flox/flox}-vil-Cre mice genetically engineered to be deficient in Paneth cells, we sought to assess the direct influence of Paneth cell antimicrobial functions on host fecal microbiota composition and subsequent consequences on intestinal pathophysiology.

Our results reveal for the first time a key role for Paneth cell-produced lysozyme on visceral sensitivity regulation through the prevention of *E. coli* expansion in intestinal microbiota.

MATERIALS AND METHODS

Mouse models

All experimental protocols described in this study were approved by the local Animal Care Use Committee (Comité d'Ethique de Pharmacologie-Toxicologie de Toulouse - Midi-Pyrénées, France) registered as N°86 at the Ministry of Research and Higher Education (N° 0029/SMVT), and conducted in accordance with the European directive 2010/63/UE. All experiments were performed on D50 mice. More details are in Supplementary Materials and Methods.

Maternal Separation protocol

To minimize cannibalism induced by perinatal stress, we used C3H/HeN mice known to be excellent breeders. Pups were separated from their dam and the rest of the litter 3 hours per day. MS was repeated for 10 working days, weekend excluded, between D2 and D15. Control pups were left with their dam (Figure S1A). More details are in Supplementary Materials and Methods.

Sox9^{flox/flox}-vil-cre mice

Heterozygote Villin-Cre (vil-Cre) mice (kindly given by S. Robine) in which the Cre recombinase is expressed specifically in the intestinal epithelium were crossed with Sox9^{flox/flox} mice (kindly given by T. Pedron), which have both *Sox9* alleles flanked by floxP sequences. This generated Sox9^{flox/flox}-vil-Cre mice, with an intestinal epithelium lacking Sox9 protein, indicating effective vil-Cre-mediated recombination of the Sox9^{flox} allele. Sox9^{flox/flox}-vil-Cre mice developed as their control littermates (Sox9^{flox/flox}).

Oral gavage of commensal *E. coli* streptomycin resistant

Live *E. coli* were isolated from feces of naïve healthy C3H/HeN mice by culture on selective ChromID coli plates (Biomérieux, Marcy L'Étoile, France). In order to facilitate monitoring of this commensal *E. coli* isolate in feces of mice after gavage, a spontaneous streptomycin resistant mutant of the commensal isolate was generated. More details are in Supplementary Materials and Methods.

Nulliparous female 35 days old C3H/HeN mice (Janvier, Roubaix, France) were randomized in two groups: vehicle, which received 100µl of bicarbonate buffer (0.2M pH8.2) *per os* per day, and *E. coli* gavage, which received 10⁹ Colony Forming Unit (CFU) of streptomycin resistant *E. coli* in 100 µl of bicarbonate buffer *per os* per day. Animals were analyzed after fifteen days of daily gavage (Figure S1B).

Lysozyme treatment

Mice submitted or not to the MS protocol received an oral gavage with lysozyme (SIGMA, ref L6876) from D35 to D50. Animals were randomized in two groups: vehicle, which received 200µl of bicarbonate buffer *per os* per day, and lysozyme gavage, which received 240 U of active lysozyme in 200 µl of bicarbonate buffer *per os* per day (Figure S1C).

Visceral sensitivity

Mice were equipped with 3 NiCr wire electrodes implanted into the abdominal external oblique muscle at D47 and kept individually after surgery. The electromyographic

(EMG) activity was recorded and analyzed with a Powerlab Chart from AD instrument. EMG recordings began 3 days after surgery. Mice were placed in polypropylene tunnels. A balloon consisting of an arterial embolectomy catheter (Fogarty, 4F, Edwards Laboratories, Santa Ana, CA) was introduced into the rectum at 2.5 cm from the anus and fixed at the base of the tail. The balloon was progressively inflated during 15 seconds by step of 0.02 ml, from 0.02 to 0.1 ml, with 10 minutes wait between each step. The Fogarty embolectomy catheter balloon was calibrated using an electronic caliper gauge and the maximal pressure applied (corresponding to 0.1 ml) was calculated as 63.1 ± 1.7 mmHg meaning that volume progressive distension corresponds to a range of pressures between 0 and 63.1 ± 1.7 mmHg. Basal EMG activity was subtracted from the EMG activity registered during the periods of distension. The use of Fogarty probe and volumes rather than barostat and pressures was selected to obtain reliable VMR at low volumes.

TNF α and IFN γ measurement in the ileum

TNF α and IFN γ were measured in supernatant on ileal fragments resuspended in RIPA buffer (0.5% deoxycholate, 0.1% SDS and 1% Igepal in TBS) containing complete anti protease cocktail (Roche), protein concentrations were measured using BCA uptima kit (Interchim).

TNF α and IFN γ concentrations were assayed using commercial enzyme linked immunosorbent assays (ELISA kits; DuoSet R&D Systems, Lille, France).

Enteric antimicrobial analysis

Lysozyme expression in Paneth cells

We used 1:100 diluted rabbit anti-mouse lysozyme antibody (Abcam, Paris, France), 0.75µg/ml Alexa fluor 488-conjugated donkey anti-rabbit IgG (Jackson, Suffolk) and 10µg/ml Alexa fluor 594-conjugated Wheat Germ Agglutinin (WGA) (Life Technology, Cergy Pontoise, France), mounted in Prolong gold antifade mounting medium with DAPI (Invitrogen) to examine lysozyme expression in Paneth cells. More details are in Supplementary Materials and Methods.

Lysozyme activity in fecal content

Activity of lysozyme against the peptidoglycan was determined in feces suspended in PBS using the EnzChek® Lysozyme Assay Kit (Molecular probes, life technology, St Aubin, France). More details are in Supplementary Materials and Methods.

Antimicrobial activity of fecal content against commensal *E. coli*

Antibacterial activity of fecal supernatant resuspended in 20% ethanol was tested against commensal *E. coli* isolated from our mice. 10^5 *E. coli* CFU grown to mid-logarithmic phase were coincubated 2h at 37°C in 10mM phosphate buffer containing 1% LB with 2mg of fecal material (20µl in 100µl final volume, 4% ethanol final so 0.2mg/ml). The resulting viable bacteria (CFU) were then enumerated by plating serial dilutions on LB agar plate incubated 24h at 37°C. The growth control was made with 4% ethanol.

Fecal microbiota composition analysis

Total community DNA was extracted from stool samples and adjusted to 1 ng/µl prior to use as described in ²⁴. Changes in the relative abundance of 21 relevant microbial 16S rRNA gene targets (supplementary method) were obtained using the GULDA platform approach ^{25,26} with minor adaptations ²⁴ described in Supplementary Materials and Methods.

The normalized N_0 -values were reported per g feces, log₁₀-transformed and processed by MixOmics package (5.2.0 version) with RStudio software (0.99.902 version) to build a partial least-squares discriminant analysis (PLS-DA)²⁷. PLS-DA is a multivariate supervised approach that operates by projecting the samples (X) onto a low-dimensional space of so-called latent variables that maximizes the separation between different groups of samples according to their class labels (Y= mice treatments). Missing normalized N_0 -values were reconstituted using the NIPALS algorithm and leave-one-out cross-validation was used to select the optimal number of latent variables for PLS-DA models with minimal error rate. Variable Importance in Projection (VIP, weighted sum of squares of the PLS loadings) scores were estimated and allowed to classify the microbial amplicon groups according to their explanatory power of class label²⁸.

Monitoring of fecal *E. coli* loads

E. coli was quantified by plating tenfold serial dilution of feces homogenates in PBS on selective ChromID coli plates (Biomérieux, Marcy L'étoile, France). For experiments of oral gavage with streptomycin resistant commensal *E. coli*, stools samples were plated on selective ChromID coli plates supplemented with 50µg/ml streptomycin. Plates were incubated at 37°C and CFU were numerated after 24 hours.

Statistical analyses

Statistical analysis was performed using GraphPad Prism version 6.0h (GraphPad Software, San Diego, California, USA). Results for single comparisons were displayed as box plots [min to max] and analyzed by performing Mann-Whitney test. Multiple groups were

displayed either as kinetics with SEM or box plots [min to max] and compared per family by Holm-Sidak's multiple comparison test or by Newman-Keuls multiple comparison test as appropriate after a significant two-way ANOVA. Differences were considered significant for $p < 0.05$.

ACCEPTED MANUSCRIPT

RESULTS

Maternal Separation (MS) in mice induced visceral hypersensitivity.

As a first step in this study, we established a MS model in C3H/HeN mice.

No weight differences were observed among groups of mice from D2 to D50.

The electromyographic (EMG) response to graded colorectal distension (CRD) was used as an index of visceral sensitivity. MS led to allodynia at day 50 in response to colorectal distension with low volume ($p=0.028$ at 0.02 ml; $p=0.007$ at 0.04 ml; $p=0.003$ at 0.06 ml compared to control; Figure 1A; representative EMG recording is presented in supplementary Figure 2A). Accordingly, Area Under the Curve (AUC) of EMG in response to increasing volumes of CRD was higher in MS mice compared to control mice ($p=0.048$; Figure 1B).

Maternal Separation (MS) reduced lysozyme expression in Paneth cells and fecal antimicrobial activity.

MS decreased ileal expression of lysozyme by Paneth cells ($p=0.0043$; Figure 2A and B) without modification of the number of crypts producing lysozyme (Figure S3). Those results differ from observations in rats where MS reduced Paneth cell number.

Moreover, fecal anti-peptidoglycan activity of lysozyme was decreased in MS mice compared to controls ($p=0.031$ of fecal proteins in control; Figure 2C). MS also decreased antimicrobial activity of fecal supernatant against commensal *E. coli* ($p=0.022$; Figure 2D). In order to assess whether MS leads to inflammation that might be responsible for visceral hypersensitivity and/or Paneth cells defect, cytokines production was measured in mice ileum.

The defect of lysozyme expression in ileal Paneth cells was associated with higher concentrations of TNF α in ileum of MS mice compared to control (p=0.033; Figure 2E) but not IFN γ (Figure 2F). Of note, myeloid cells as source for the elevated TNF α concentrations in ileum had been considered but immunofluorescence of lysozyme positive cells did not provide evidence for an influx of myeloid cells as shown in Figure S4. Furthermore, no modification of IL17 nor IL22 nor IL10 concentration was observed in response to MS in ileum (Figure S5).

Loss of Paneth cells in Sox9^{flox/flox}-vil-cre mice was associated with visceral hypersensitivity.

Sox9^{flox/flox}-vil-cre mice presenting a decrease of the goblet cell lineage and an absence of Paneth cells^{29,30} displayed visceral hypersensitivity at day 50 mimicking the effect observed in MS mice. Indeed, Sox9^{flox/flox}-vil-cre mice responded with higher EMG activity to colorectal distension at the volume of 0.04 ml compared to littermate Sox9^{flox/flox} (p=0.0014; Figure 3A). Representative EMG recording is presented in supplementary Figure 2B. More generally, AUC of EMG activity in response to increasing volumes of distension was higher in Sox9^{flox/flox}-vil-cre mice compared to littermate (p=0.021; Figure 3B).

Paneth cell depletion in Sox9^{flox/flox}-vil-cre mice led to a smaller antimicrobial activity of fecal supernatant against commensal *E. coli* (p=0.01, Figure 3C). However, no modification of TNF α concentrations was observed in ileum of Sox9^{flox/flox}-vil-cre compared to littermate mice (Figure 3D).

Both C3H/HeN submitted to MS and Sox9^{flox/flox}-vil-cre mice induced fecal dysbiosis characterized by an expansion of *E. coli* positively correlated with visceral hypersensitivity.

Based on measurement of the relative abundance of 21 microbial taxa in feces, two distinct partial least-squares discriminant analysis (PLS-DA) were built to depict fecal microbial signature associated with MS (Figure 4A) and Paneth cell depletion in Sox9^{flox/flox}-vil-cre (Figure 4B). Both score plots revealed a separation of microbial mice profile according to MS and genotype respectively. Associated VIP scores (Figure 4C and D) allowed to rank key microbial phylotypes based on their importance in discrimination between mouse groups. Fecal microbial signature associated with MS consisted in an increase of the relative abundances of *Methanobrevibacter smithii* (p=0.028), *Ruminococcus gnavus* (p=0.043), *Eubacterium hallii* (p=0.18) and *E. coli* (p=0.1) associated with a decrease of the *Roseburia* at the genus level (p=0.36) (Figure 4C, Figure S6). Increase of the relative abundances of *Bacteroides fragilis* (p=0.0014) and *E. coli* (p= 0.041) (Figure 4D) in Sox9^{flox/flox}-vil-cre mice was accompanied by a global increase of bacteria mainly belonging to Bacteroidetes phylum (*Bacteroides spp.* and *Prevotella spp.*, p=0.05 and p=0.019 respectively) and *Enterococcus spp.* and a decrease of relative abundance of *Bifidobacterium spp.* (Figure 4D, Figure S7).

Among the main contributors to dysbiosis (VIP>1), fecal *E. coli* expansion represents a common feature associated with MS and Paneth cell defect in Sox9^{flox/flox}-vil-cre mice. These qPCR-based analyzes of the relative abundance of *E. coli* (Figure 5A and 5B) were confirmed using bacterial culture. Increase of *E. coli* abundance was indeed observed by plating fecal pellet on selective agar in feces of mice submitted to MS (Figure 5C, p=0.0002) and Sox9^{flox/flox}-vil-cre mice (Figure 5D, p=0.042).

E. coli increase in MS and Sox9^{flox/flox}-vil-cre positively correlated with high AUC of EMG attesting of visceral hypersensitivity (Figure 5E and F).

***E. coli* gavages induced fecal dysbiosis associated with visceral hypersensitivity without inflammation**

By comparing key microbial features (VIP) previously identified as important in discrimination of mouse microbiota according to their antimicrobial activity, we noted that *E. coli* expansion was observed in both mouse models (MS and Sox9^{flox/flox}-vil-cre mice.) We wondered if the defect in Paneth cells associated with fecal dysbiosis in favor of *E. coli* could be responsible for the observed visceral hypersensitivity. To answer this question, C3H/HeN mice was submitted to 15 days of oral gavage with an autochthonous commensal *E. coli* resistant for streptomycin in order to follow its implantation (Figure S1B). After 15 days of gavage, streptomycin resistant *E. coli* represented 90% of fecal *E. coli* as enumerated on ChromID agar plates supplemented or not with 50µg/ml streptomycin.

Variance in selected fecal microbial taxa abundances discriminated daily *E. coli* fed mice compared with vehicle treated mice (Figure 6A). As expected, *E. coli* was the most important contributor responsible for difference observed in microbial profile of mice (Figure 6B). Increase of relative abundance of fecal *E. coli* was observed on mice after oral gavage by plating fecal pellet on ChromID agar (p=0.0007; Figure 6C) and by qPCR (p=0.017; Figure 6D).

The resulting dysbiosis in favor of *E. coli* induced visceral hypersensitivity in response to colorectal distension at the volume of 0.04 ml (p=0.017) and 0.06 ml (p=0.0003; Figure 6E). Representative EMG recording is presented in supplementary Figure 2C. More generally,

AUC of EMG activity in response to increasing volumes of distension was higher in mice submitted to *E. coli* oral gavage compared to vehicle-treated mice ($p=0.002$; Figure 6F).

E. coli gavage did not trigger ileal inflammation as TNF α ileal concentrations remained unchanged after *E. coli* gavages (Figure 6G) and no modification of IFN γ was observed (data not shown).

Oral treatment of young MS mice with lysozyme prevented stress-induced *E. coli* expansion and associated visceral hypersensitivity in adult.

We wondered if an oral supplementation of MS mice with lysozyme could conversely prevent *E. coli* expansion and visceral hypersensitivity. Daily oral gavage of MS mice with 240U of lysozyme from day 35 to day 50 (Figure S1C) was performed. By plating fecal pellet on selective agar at day 35, no difference in *E. coli* counting was observed between MS and control (data not shown). Fifteen days of lysozyme treatment of MS mice prevented fecal increase of *E. coli* ($p<0.001$; Figure 7A).

However, increase of TNF α in ileum of MS mice was not prevented by lysozyme treatment ($p<0.05$; Figure 7B).

Lysozyme treatment also prevented visceral hypersensitivity in 50 days old adult MS mice ($p<0.0045$ at 0,04 ml; $p<0.0001$ at 0.06ml; $p<0.0001$ at 0.08 ml; Figure 7C). Representative EMG recording is presented in supplementary Figure 2A. Accordingly, AUC of EMG activity in response to increasing volumes of distension was higher in MS mice compared to MS mice orally treated with lysozyme ($p=0.0006$; Figure 7D).

Discussion

Paneth cells producing enteric antimicrobial peptides are important players in small intestine innate immunity. In mice, Paneth cells appear only 2 weeks after birth³¹⁻³⁴ and they are sensitive to environmental factors including enteric infections^{35,36} and early life stress²². Indeed, MS performed in rat decreases epithelial secretory cell lineages number including Paneth cells²². Furthermore, neonatal maternal separation (MS) induces visceral hypersensitivity at adulthood²³. This observation questioned a potential role of Paneth cell defect triggered by an environmental factor like MS in the induction of visceral hypersensitivity.

In the mice model of MS established in this study, we show that MS impaired Paneth cell functions attested by a decrease of lysozyme expression but not the number of Paneth cells as observed in rats. We also demonstrated that impaired Paneth cell functionality induced by maternal separation or Paneth cell deficiency in genetic engineered Sox9^{flox/flox}-vil-Cre mice led to fecal dysbiosis in favor of *E. coli* and visceral hypersensitivity in response to colorectal distension.

Regarding these results, we wondered if the observed defect of lysozyme expression in Paneth cells in MS mice might be responsible for visceral hypersensitivity. To answer this question, Sox9^{flox/flox}-vil-Cre mice deficient for Paneth cells were used. Visceral hypersensitivity in response to colorectal distension was observed in Sox9^{flox/flox}-vil-Cre mice compared to littermate Sox9^{flox/flox} mimicking the phenotype of MS mice. Then, we aimed at deciphering the mechanisms by which Paneth cell defect can induce visceral hypersensitivity.

The role of Paneth cells derived antimicrobial compounds is not limited to the small intestine where they are produced and secreted but they also act in lumen of caecum and colon³⁷⁻³⁹.

Consequently, we undertook to address the consequences of Paneth cell defect in Sox9^{flox/flox}-vil-Cre mice and MS mice on fecal microbiota. Interestingly, both mice models MS and Sox9^{flox/flox}-vil-Cre mice developed a dysbiosis and the common hallmark of this dysbiosis was a specific increase of *E. coli*, a representative strain of *Enterobacteriaceae* family. This characterization was obtained by performing the previously described GUt Low Density Array platform²⁵, and confirmed by bacterial culture. The qPCR GULDA method used only focused on luminal microbiota. A potential involvement of adherent bacteria in MS-induced dysbiosis was therefore questioned and in particular the role of Segmented Filamentous Bacteria (SFB), a representative adherent bacteria known to be a strong inducer of Th17 response in intestinal lamina propria^{40,41}. MS did not induce any modification of IL17 production in ileum suggesting no major modification of SFB population by MS.

E. coli expansion in both mouse models (MS and Sox9^{flox/flox}-vil-Cre mice) is in agreement with literature showing in various rodent models that impaired Paneth cell functions potentiate *Enterobacteriaceae* growth. Defects in Paneth cell granule composition including lysozyme observed in Cd1d^{-/-} mice result in *E. coli* expansion not only in small intestine content, but also in feces⁴². In the mouse graft-versus-host disease (GVHD) model inducing Paneth cell defect in number and function, a reduced diversity of the fecal microbiota is observed, as well as an overwhelming expansion of *E. coli* leading to GVHD mice death due to *E. coli*-induced septicemia⁴³. Finally, dithizone-induced Paneth cell depletion is detrimental to host defense against *E. coli* infection in rat neonatal small intestine⁴⁴. Interestingly, previous works showed that MS induces microbiota dysbiosis in favor of coliforms in rats⁴⁵ and monkeys⁴⁶. Finally, in 8 week old rats, MS induced microbiota dysbiosis characterized by reduced diversity and higher representation of Proteobacteria phylum (including *Enterobacteriaceae* family)⁴⁷. All these data strongly support the role of Paneth cells in control of *E. coli* population in small and large intestine.

E. coli expansion in our models of Paneth cell defect (MS and Sox9^{flox/flox}-vil-Cre) was observed without a broader microbiota overgrowth (Figure S8). This is in agreement with previous studies showing that Paneth cell defect induced microbial dysbiosis occurs without microbiota overgrowth^{5,48}.

Interestingly, in both models, MS and Sox9^{flox/flox}-vil-Cre a strong positive correlation was observed between *E. coli* fecal CFU and AUC of EMG attesting of visceral sensitivity. Next, we aimed to decipher if visceral hypersensitivity triggered by Paneth cell genetic or functional defect in Sox9^{flox/flox}-vil-Cre and MS mice respectively was a consequence of *E. coli* expansion. Fifteen days of oral gavage on conventional mice with autochthonous *E. coli* induced fecal *E. coli* expansion and visceral hypersensitivity, showing that the *E. coli* expansion is responsible for the visceral hypersensitivity occurrence. Interestingly, early life vancomycin treated rats displayed an increase in *Proteobacteria* associated with visceral hypersensitivity at adulthood⁴⁹. Here, we further dissected the mechanism and demonstrated for the first time that *E. coli*, a member of this phylum, is responsible for visceral hypersensitivity.

The mechanism involved in Paneth cell functional defect observed in MS model is still unknown. As, TNF α is known to damage Paneth cells⁵⁰, one can hypothesizes that MS-induced ileal inflammation attested by an increase in ileal TNF α concentration may be responsible for Paneth cell dysfunction. However, the source of the increased TNF α concentration is still unknown and will warrant further investigations. In this study we have not observed changes in ileal concentrations of other pro-inflammatory cytokines known to impair Paneth cells such as IFN γ ³⁶. On the other hand, the ileal increase of TNF α was only observed in the MS model but neither in Sox9^{flox/flox}-vil-Cre mice nor in mice receiving *E. coli* by oral gavage excluding a direct role of TNF α in the visceral hypersensitivity observed in these different models.

Thereafter, we undertook to clarify the link between the Paneth cell functional defect, namely the decrease of lysozyme expression in the MS model and the associated *E. coli* expansion. In our MS model on mice, Paneth cell function defect was attested by a decrease of lysozyme expression. However, lysozyme is not the only antimicrobial compound produced by Paneth cells. Indeed, Paneth cells produce and secrete other antimicrobial proteins or peptides (AMP) like phospholipase A2 (PLA2), Reg3 lectins and α -defensin (for review ⁴). Nevertheless, lysozyme oral treatment could prevent MS-induced *E. coli* overgrowth and visceral hypersensitivity. Prevention of *E. coli* expansion by LZM treatment is either the result of LZM anti-microbial activity against *E. coli* or indirectly, a modification of microbiota composition repressing *E. coli* expansion. Neither the less LZM treatment results in preventing *E. coli* overgrowth and visceral hypersensitivity induced by MS. Interestingly, lysozyme oral treatment prevented MS-induced *E. coli* expansion but not TNF α increase in ileum suggesting that inflammation driven by TNF α release may be responsible for Paneth cell defect and *E. coli* expansion and not the opposite i.e. *E. coli* overwhelming inducing intestinal inflammation. This claim is supported by studies demonstrating that intestinal inflammation boosts *E. coli* growth ⁵¹. Furthermore, De Palma et al. demonstrated that MS-induced changes in host physiology are the cause of intestinal dysbiosis and not the opposite. Indeed, control mice receiving MS mouse dysbiotic microbiota by oral gavage were not able to maintain this microbiota and failed to develop anxiety-like behavior observed in MS mice ⁵².

Interestingly, even though mouse gut microbiota is strain-specific ⁸, *E. coli* expansion was observed in both tested models of Paneth cell deficiency: MS in C3H/HeN mice and genetic engineered intestinal depletion of *Sox9* in C57BL/6 strain. *E. coli* expansion due to Paneth cell number and function defects has also been observed independently of mouse genetic background in a model of GVHD ⁴³. Those observations highlight the major role of Paneth

cells in controlling *E. coli* intestinal population independently of mouse strain and mouse antimicrobial repertoire^{8,9}.

Taken together the results of this study showed that (i) both MS mice and Sox9^{flox/flox}-vil-Cre mice exhibit fecal *E. coli* expansion and visceral hypersensitivity, (ii) oral gavage of conventional mice with *E. coli* induces fecal *E. coli* increase and visceral hypersensitivity and (iii) lysozyme oral treatment of MS mice can prevent *E. coli* fecal expansion and visceral hypersensitivity, we propose the following cascade of events: the Paneth cells antimicrobial defect induces microbiota dysbiosis characterized mainly by *E. coli* population expansion, responsible for visceral hypersensitivity in response to colorectal distension.

From a clinical point of view, the findings reported in this study are of particular importance and highlight the role of Paneth cells in shaping intestinal microbiota and its consequences on visceral hypersensitivity. For the first time, we establish a cause-effect relationship between Paneth cell-induced dysbiosis and visceral hypersensitivity in preclinical models. Our results raise the interesting possibility that Paneth cells may be an important player in the pain symptomatology of a variety of multifactorial organic (CD) and functional (IBS) gastrointestinal diseases sharing at least three common features: visceral hypersensitivity, microbiota dysbiosis and stress as contributor to the pathology. The allodynic response to colorectal distension observed in MS mice enhances the relevance of our data in IBS pathophysiology, since IBS patients exhibit lower discomfort and visceral pain thresholds to colorectal distension compared to healthy controls⁵³⁻⁵⁵. Furthermore, it has been described that intestinal tissues from NEC infants have fewer LZM-producing intestinal cells compared with healthy infants¹³ and that NEC incidence is decreased in breast fed infant⁵⁶. In a pig model producing human LZM in milk, human LZM milk can inhibit *E. coli* growth in small intestine of suckling piglet⁵⁷ highlighting the role of LZM in controlling *E. coli* expansion.

REFERENCES

1. Bäckhed F, Ley RE, Sonnenburg JL, et al. Host-bacterial mutualism in the human intestine. *Science* 2005;307:1915–20. Available at: <http://www.sciencemag.org/cgi/doi/10.1126/science.1104816><http://www.ncbi.nlm.nih.gov/pubmed/15790844>.
2. Gill S, Pop M, DeBoy R, et al. Metagenomic analysis of the human distal gut microbiome. *Science* (80-) 2006;312:1355–1359. Available at: <http://www.sciencemag.org/content/312/5778/1355.short>.
3. Turnbaugh PJ, Ley RE, Hamady M, et al. Feature The Human Microbiome Project. *Nature* 2007;449:804–810.
4. Bevins CL, Salzman NH. Paneth cells, antimicrobial peptides and maintenance of intestinal homeostasis. *Nat Rev Microbiol* 2011;9:356–368. Available at: <http://dx.doi.org/10.1038/nrmicro2546>.
5. Salzman NH, Hung K, Haribhai D, et al. Enteric defensins are essential regulators of intestinal microbial ecology. *Nat Immunol* 2010;11:76–83. Available at: <http://dx.doi.org/10.1038/ni.1825>.
6. Brandl K, Plitas G, Schnabl B, et al. MyD88-mediated signals induce the bactericidal lectin RegIII γ and protect mice against intestinal *Listeria monocytogenes* infection. *J Exp Med* 2007;204:1891–1900. Available at: <http://www.pubmedcentral.nih.gov/articlerender.fcgi?artid=2118673&tool=pmcentrez&rendertype=abstract><http://www.jem.org/lookup/doi/10.1084/jem.20070563>.
7. Wilson CL. Regulation of Intestinal γ -Defensin Activation by the Metalloproteinase Matrilysin in Innate Host Defense. *Science* (80-) 1999;286:113–117. Available at: <http://www.sciencemag.org/cgi/doi/10.1126/science.286.5437.113>.

8. Gulati AS, Shanahan MT, Arthur JC, et al. Mouse background strain profoundly influences paneth cell function and intestinal microbial composition. *PLoS One* 2012;7.
9. Shanahan MT, Tanabe H, Ouellette AJ. Strain-specific polymorphisms in paneth cell α -defensins of C57BL/6 mice and evidence of vestigial myeloid α -defensin pseudogenes. *Infect Immun* 2011;79:459–573.
10. Pütsep K, Axelsson LG, Boman A, et al. Germ-free and colonized mice generate the same products from enteric prodefensins. *J Biol Chem* 2000;275:40478–40482.
11. Hooper L V, Gordon JI. Commensal host-bacterial relationships in the gut. *Science* 2001;292:1115–1118.
12. O’Neil D a, Porter EM, Elewaut D, et al. Expression and regulation of the human beta-defensins hBD-1 and hBD-2 in intestinal epithelium. *J Immunol* 1999;163:6718–6724.
13. Coutinho HB, Mota HC da, Coutinho VB, et al. Absence of lysozyme (muramidase) in the intestinal Paneth cells of newborn infants with necrotising enterocolitis. *J Clin Pathol* 1998;51:512–514.
14. Wehkamp J, Harder J, Weichenthal M, et al. NOD2 (CARD15) mutations in Crohn’s disease are associated with diminished mucosal alpha-defensin expression. *Gut* 2004;53:1658–64. Available at: <http://www.ncbi.nlm.nih.gov/pubmed/15479689> <http://www.pubmedcentral.nih.gov/articlerender.fcgi?artid=PMC1774270>.
15. Wehkamp J. Reduced Paneth cell α -defensins in ileal Crohn’s disease. *Proc Natl Acad Sci* 2005;102:18129–18134.
16. Halfvarson J. Genetics in twins with Crohn’s disease: Less pronounced than previously believed? *Inflamm Bowel Dis* 2011;17:6–12.
17. Schreiber S, Rosenstiel P, Albrecht M, et al. Genetics of Crohn disease, an archetypal inflammatory barrier disease. *Nat Rev Genet* 2005;6:376–388.

18. Halpin SJ, Ford AC. Prevalence of symptoms meeting criteria for irritable bowel syndrome in inflammatory bowel disease: systematic review and meta-analysis. *Am J Gastroenterol* 2012;107:1474–82. Available at: <http://dx.doi.org/10.1038/ajg.2012.260>.
19. Chang C, Lin H. Dysbiosis in gastrointestinal disorders. *Best Pract Res Clin Gastroenterol* 2016;30:3–15.
20. Videlock EJ, Adeyemo M, Licudine A, et al. Childhood Trauma Is Associated With Hypothalamic-Pituitary-Adrenal Axis Responsiveness in Irritable Bowel Syndrome. *Gastroenterology* 2009;137:1954–1962.
21. Wegman HL, Stetler C. A meta-analytic review of the effects of childhood abuse on medical outcomes in adulthood. *Psychosom Med* 2009;71:805–812.
22. Estienne M, Claustre J, Clain-Gardechaux G, et al. Maternal deprivation alters epithelial secretory cell lineages in rat duodenum: role of CRF-related peptides. *Gut* 2010;59:744–751.
23. Barreau F, Ferrier L, Fioramonti J, et al. Neonatal maternal deprivation triggers long term alterations in colonic epithelial barrier and mucosal immunity in rats. *Gut* 2004;53:501–6. Available at: <http://www.pubmedcentral.nih.gov/articlerender.fcgi?artid=1774003&tool=pmcentrez&rendertype=abstract>.
24. Yvon S, Olier M, Leveque M, et al. Donkey milk consumption exerts anti-inflammatory properties by normalizing antimicrobial peptides levels in Paneth's cells in a model of ileitis in mice. *Eur J Nutr* 2016. Available at: <http://link.springer.com/10.1007/s00394-016-1304-z>.
25. Bergström A, Licht TR, Wilcks A, et al. Introducing GUT Low-Density Array (GULDA) - a validated approach for qPCR-based intestinal microbial community analysis. *FEMS Microbiol Lett* 2012;337:38–47.

26. Bergström A, Skov TH, Bahl MI, et al. Establishment of intestinal microbiota during early life: A longitudinal, explorative study of a large cohort of Danish infants. *Appl Environ Microbiol* 2014;80:2889–2900.
27. Dejea S, Gonzalez I, With K-ALC. Omics Data Integration Projec. *R Packag version* 2012;5.0:3.
28. Tenenhaus M. *La regression PLS:theorie et pratique*. Technip Ed. Paris; 1998.
29. Mori-Akiyama Y, Born M van den, Es JH van, et al. SOX9 Is Required for the Differentiation of Paneth Cells in the Intestinal Epithelium. *Gastroenterology* 2007;133:539–546.
30. Bastide P, Darido C, Pannequin J, et al. Sox9 regulates cell proliferation and is required for Paneth cell differentiation in the intestinal epithelium. *J Cell Biol* 2007;178:635–648.
31. Es JH van, Jay P, Gregorieff A, et al. Wnt signalling induces maturation of Paneth cells in intestinal crypts. *Nat Cell Biol* 2005;7:381–386.
32. Bry L, Falk P, Huttner K, et al. Paneth cell differentiation in the developing intestine of normal and transgenic mice. *Proc Natl Acad Sci U S A* 1994;91:10335–10339.
33. Ménard S, Förster V, Lotz M, et al. Developmental switch of intestinal antimicrobial peptide expression. *J Exp Med* 2008;205:183–93. Available at: <http://jem.rupress.org/content/205/1/183.full>.
34. Darmoul D, Ouellette AJ. Positional specificity of defensin gene expression reveals Paneth cell heterogeneity in mouse small intestine. *Am J Physiol* 1996;271:G68–G74.
35. Rodriguez NRM, Eloi MD, Huynh A, et al. Expansion of paneth cell population in response to enteric salmonella enterica serovar typhimurium infection. *Infect Immun* 2012;80:266–275.
36. Raetz M, Hwang S-H, Wilhelm CL, et al. Parasite-induced TH1 cells and intestinal

- dysbiosis cooperate in IFN- γ -dependent elimination of Paneth cells. *Nat Immunol* 2013;14:136–42. Available at: <http://www.ncbi.nlm.nih.gov/pubmed/23263554> <http://www.pubmedcentral.nih.gov/articlerender.fcgi?artid=PMC3552073>.
37. Mastroianni JR, Ouellette AJ. α -Defensins in enteric innate immunity. Functional paneth cell α -defensins in mouse colonic lumen. *J Biol Chem* 2009;284:27848–27856.
 38. Mastroianni JR, Costales JK, Zaksheske J, et al. Alternative luminal activation mechanisms for paneth cell alpha-defensins. *J Biol Chem* 2012;287:11205–11212.
 39. Nakamura K, Sakuragi N, Ayabe T. A monoclonal antibody-based sandwich enzyme-linked immunosorbent assay for detection of secreted alpha-defensin. *Anal Biochem* 2013;443:124–131.
 40. Ivanov II, Atarashi K, Manel N, et al. Induction of Intestinal Th17 Cells by Segmented Filamentous Bacteria. *Cell* 2009;139:485–498.
 41. Gaboriau-Routhiau V, Rakotobe S, Lecuyer E, et al. The Key Role of Segmented Filamentous Bacteria in the Coordinated Maturation of Gut Helper T Cell Responses. *Immunity* 2009;31:677–689.
 42. Nieuwenhuis EES, Matsumoto T, Lindenbergh D, et al. Cd1d-dependent regulation of bacterial colonization in the intestine of mice. *J Clin Invest* 2009;119:1241–1250.
 43. Eriguchi Y, Takashima S, Oka H, et al. Graft-versus-host disease disrupts intestinal microbial ecology by inhibiting Paneth cell production of alpha-defensins. *Blood* 2012;120:223–231.
 44. Sherman MP, Bennett SH, Hwang FFY, et al. Paneth cells and antibacterial host defense in neonatal small intestine. *Infect Immun* 2005;73:6143–6146.
 45. O'Mahony SM, Marchesi JR, Scully P, et al. Early Life Stress Alters Behavior, Immunity, and Microbiota in Rats: Implications for Irritable Bowel Syndrome and

- Psychiatric Illnesses. *Biol Psychiatry* 2009;65:263–267.
46. Bailey MT, Coe CL. Maternal separation disrupts the integrity of the intestinal microflora in infant rhesus monkeys. *Dev Psychobiol* 1999;35:146–155.
47. Zhou X-Y. Visceral hypersensitive rats share common dysbiosis features with irritable bowel syndrome patients. *World J Gastroenterol* 2016;22:5211. Available at: <http://www.wjgnet.com/1007-9327/full/v22/i22/5211.htm>.
48. Vaishnava S, Behrendt CL, Ismail AS, et al. Paneth cells directly sense gut commensals and maintain homeostasis at the intestinal host-microbial interface. *Proc Natl Acad Sci* 2008;105:20858–20863. Available at: <http://www.pnas.org/cgi/doi/10.1073/pnas.0808723105>.
49. O'Mahony SM, Felice VD, Nally K, et al. Disturbance of the gut microbiota in early-life selectively affects visceral pain in adulthood without impacting cognitive or anxiety-related behaviors in male rats. *Neuroscience* 2014;277:885–901.
50. Hauwermeiren F Van, Vandenbroucke RE, Grine L, et al. TNFR1-induced lethal inflammation is mediated by goblet and Paneth cell dysfunction. *Mucosal Immunol* 2014:1–13. Available at: <http://www.ncbi.nlm.nih.gov/pubmed/25425265>.
51. Winter SE, Winter MG, Xavier MN, et al. Host-derived nitrate boosts growth of *E. coli* in the inflamed gut. *Science* 2013;339:708–11. Available at: <http://www.ncbi.nlm.nih.gov/pubmed/23393266>.
52. Palma G De, Blennerhassett P, Lu J, et al. Microbiota and host determinants of behavioural phenotype in maternally separated mice. *Nat Commun* 2015;6:7735. Available at: <http://www.nature.com/doi/10.1038/ncomms8735>.
53. Chang L, Mayer E a, Labus JS, et al. Effect of sex on perception of rectosigmoid stimuli in irritable bowel syndrome. *Am J Physiol Regul Integr Comp Physiol* 2006;291:R277-84.

54. Bradette M, Delvaux M, Staumont G, et al. Evaluation of colonic sensory thresholds in IBS patients using a barostat. Definition of optimal conditions and comparison with healthy subjects. *Dig Dis Sci* 1994;39:449–457.
55. Ludidi S, Conchillo JM, Keszthelyi D, et al. Rectal hypersensitivity as hallmark for irritable bowel syndrome: Defining the optimal cutoff. *Neurogastroenterol Motil* 2012;24.
56. Lucas A, Cole TJ. Breast milk and neonatal necrotising enterocolitis. *Lancet* 1990;336:1519–1523.
57. Lu D, Li Q, Wu Z, et al. High-level recombinant human lysozyme expressed in milk of transgenic pigs can inhibit the growth of *Escherichia coli* in the duodenum and influence intestinal morphology of sucking pigs. *PLoS One* 2014;9.

Legends

Figure 1 – Visceral sensitivity on maternally separated (MS) adult mice. (A) Representative curves of electromyograph (EMG) in response to colorectal distension with increasing volumes (0.02 to 0.1ml) in MS (grey squares plain line) compared to control (white circles dashed line) (n = 12 to 21 mice per group). * P<0,05 and ** P<0,01 compared to control (Two-way ANOVA followed by Holm-Sidak's post-test). (B) Responses to colorectal distension are depicted as Area Under the Curve (AUC) (n = 12 to 21 mice per group). * P<0,05 compared to identical volumes for controls (Mann-Whitney test).

Figure 2 - Antimicrobial response on maternally separated (MS) adult mice. (A) Immunostaining of ileum paraffin section with anti-lysozyme-(FITC), Wheat germ agglutinin (WGA)-Texas red and DAPI. (B) Lysozyme fluorescence intensity per crypt cell in MS (grey) compared to control (white) (n = 5 – 6 mice per group). ** P<0,01 compared to control. (C) Enzymatic activity of lysozyme against peptidoglycan in feces supernatants (n = 7 to 9 mice per group). * P<0,05 compared to control. (D) Fecal antimicrobial activity against commensal *E. coli* (fecal protein concentration: 20mg/ml) (n = 9 - 10 mice per group). *: P<0.05 compared control. (E) TNF α concentration in the ileum fragment measured by ELISA (n = 15 to 17 mice per group). * P<0.05 compared control. (F) IFN γ concentration in the ileum fragment measured by ELISA (n = 8 to 9 mice per group). (Mann-Whitney test).

Figure 3 – Visceral sensitivity on adult Sox9^{flox/flox}-vil-cre mice. (A) Representative curves of EMG in response to colorectal distension with increasing volumes (0.02 to 0.1ml) in Sox9^{flox/flox}-vil-cre (grey square plain line) compared to littermate (white circle dashed line) (n = 14 to 15 mice per group). ** P<0,01 compared to identical volumes for controls. (Two-way ANOVA followed by Holm-Sidak's post-test) (B) Responses to colorectal distension are

depicted as AUC (n = 14 to 15 mice per group). * P<0,05 compared to littermate (C) Fecal antimicrobial activity against commensal *E. coli* (fecal protein concentration: 20 mg/ml) (n = 9 to 10 mice per group) * P<0,05 compared to littermate. (D) TNF α concentration in the ileum fragment measured by ELISA (n = 14 to 15 mice per group). (Mann-Whitney test).

Figure 4 - Fecal microbiota analysis on maternally separated (MS) and Sox9^{flox/flox}-vil-cre adult mice. PLS-DA score plot of the relative quantitative abundances (Log₁₀ No) of 21 microbial taxa in feces of MS and control mice (n= 10 mice per group, confidence ellipse level =0.5) (A) and of Sox9^{flox/flox}-vil-cre mice and littermate (n= 10 mice per group, confidence ellipse level =0.5) (B). VIP plot representing important features (microbial taxa) identified by PLS-DA in a descending order of importance (Increase of relative abundances appeared in red and decrease in green) in MS and control mice (C) and in Sox9^{flox/flox}-vil-cre mice and littermate (D).

Figure 5 – Fecal *E. coli* analysis on maternally separated (MS) and Sox9^{flox/flox}-vil-cre adult mice correlated with AUC of EMG. Relative abundances per g feces of *E. coli* by real-time qPCR in MS and control mice (A) and Sox9^{flox/flox}-vil-cre mice and littermate (B) (n= 9 – 10 mice per group) *: P<0.05 compared to littermate. Counting of *E. coli* colonies on ChromID coli selective plates reported per g feces in MS and control mice (n = 8 mice per group) ***: P<0.001 compared to control (C) and Sox9^{flox/flox} vil-cre mice and littermate (n= 11 to 13 mice per group) *: P<0.05 compared to littermate (D). (Mann-Whitney test).

Correlation between *E. coli* CFU and AUC of EMG of control and MS mice (Pearson r=0.6949, P=0.0028) (E) and littermate and Sox9^{flox/flox}-vil-cre (Pearson r=0.5513, P=0.0331) (F).

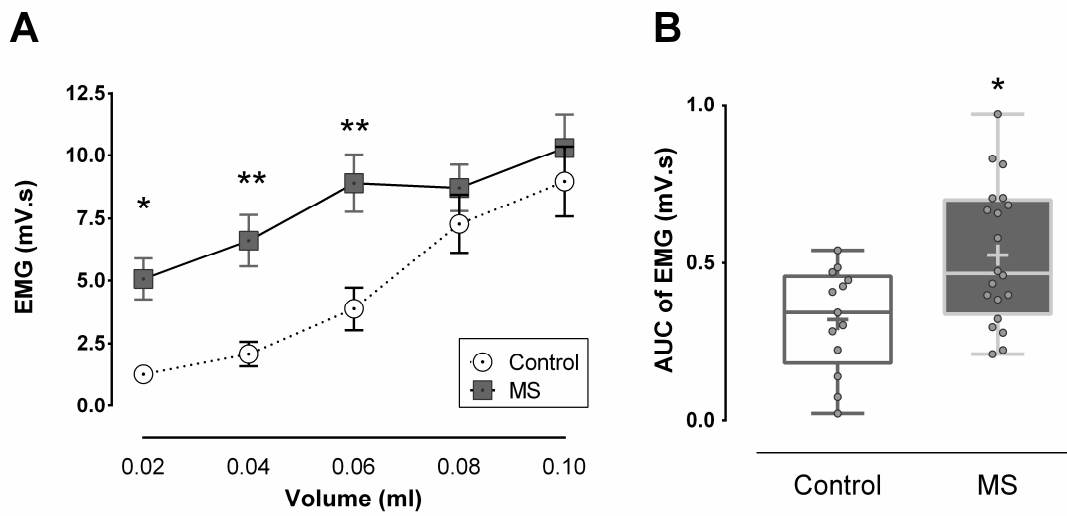
Figure 6 - Fecal microbiota, inflammation and visceral sensitivity analysis on adult mice receiving commensal *E. coli* by oral gavage. (A) PLS-DA score plot of the relative

quantitative abundances (Log10 No) of 21 microbial taxa in feces of mice receiving commensal *E. coli* or vehicle by oral gavage (n= 10 mice per group, confidence ellipse level =0.5). **(B)** VIP plot representing important features (microbial taxa) identified by PLS-DA in a descending order of importance (Increase of relative abundances appeared in red and decrease in green). **(C)** Counting of fecal *E. coli* colonies on ChromID coli selective plates after 15 days of oral gavage with *E. coli*. (n = 11 - 12 mice per group) ***: P<0.001 compared to control. (Mann-Whitney test) **(D)** Relative abundances per g feces of *E. coli* by real-time PCR (n = 10 - 11 mice per group) *: P<0.05 compared to control. (Mann-Whitney test) **(E)** Representative curves of EMG in response to colorectal distension with increasing volumes (0.02 to 0.1ml) in mice receiving *E. coli* by oral gavage (grey squares plain line) compared to control/vehicle (white circles dashed line) (n = 8 mice per group). **: P<0,01 and ***: P<0.001 compared to identical volumes for controls. (Two-way ANOVA followed by Holm-Sidak's post-test). **(F)** Responses to colorectal distension are depicted as Area Under the Curve (AUC) (n = 8 mice per group). ***: P<0,001 compared to vehicle. **(G)** TNF α concentration in the ileum fragment measured by ELISA (n = 10 to 11 mice per group). (Mann-Whitney test).

Figure 7 - Fecal microbiota, inflammation and visceral sensitivity analysis on MS adult mice orally treated or not with lysozyme for 15 days. **(A)** Counting of *E. coli* colonies on ChromID selective plates after 15 days of oral lysozyme treatment (D50/G15) (n = 14 to 15 mice per group). *: P<0,05 compared to controls; $\mu\mu\mu$: P<0.001 compared to MS+LZM; #: P<0.05 compared to control+LZM; ##: P<0.01 compared to control+LZM. controls. (Two-way ANOVA followed by Newman-keuls post-test). **(B)** TNF α concentration in the ileum fragment measured by ELISA (n = 14 to 22 mice per group). *P<0.05 compared to control. (Two-way ANOVA followed by Newman-keuls post-test). **(C)** Representative curves of EMG in response to colorectal distension with increasing volumes (0.02 to 0.1ml) in MS

(grey square), MS treated with LZM (pale grey squares), control (white circles) and control treated with LZM (grey circles) (n = 8-9 mice per group). *: P<0,05 compared to identical volumes for controls; ** P<0,01 compared to identical volumes for controls; *** P<0,001 compared to identical volumes for controls; $\mu\mu$: P<0.01 compared to MS+LZM; $\mu\mu\mu$: P<0.001 compared to MS+LZM; ## P<0.01 compared to control+LZM; ### P<0.001 compared to control+LZM. (Two-way ANOVA followed by Holm-Sidak's post-test) **(D)** Responses to colorectal distension are depicted as AUC (n = 8 - 9 mice per group). ***: P<0,001 compared to control; $\mu\mu\mu$: p<0.001 compared to MS+LZM and # p<0.05 compared to control+LZM. (Two-way ANOVA followed by Holm-Sidak's post-test).

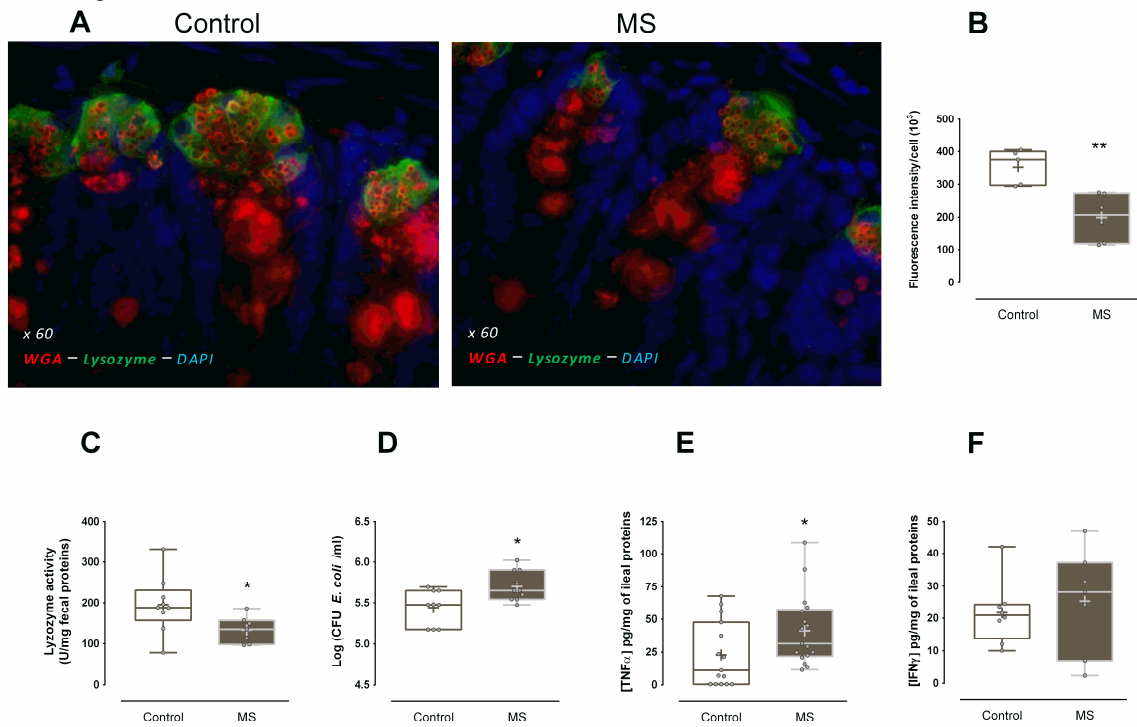
Figure 1



Comment citer ce document :

Riba, A., Olier, M., Lacroix Lamandé, S., Lencina, C., Bacquié, V., Harkat, C., Gillet, M., Baron, M., Sommer, C., Mallet, V., Salvador Cartier, C., Laurent, F., Théodorou, V., Ménard, S. (2017). Paneth cell defects induce microbiota dysbiosis in mice and promote visceral hypersensitivity. *Gastroenterology*. 153 (6). 1594-1606. DOI : 10.1053/j.gastro.2017.08.044

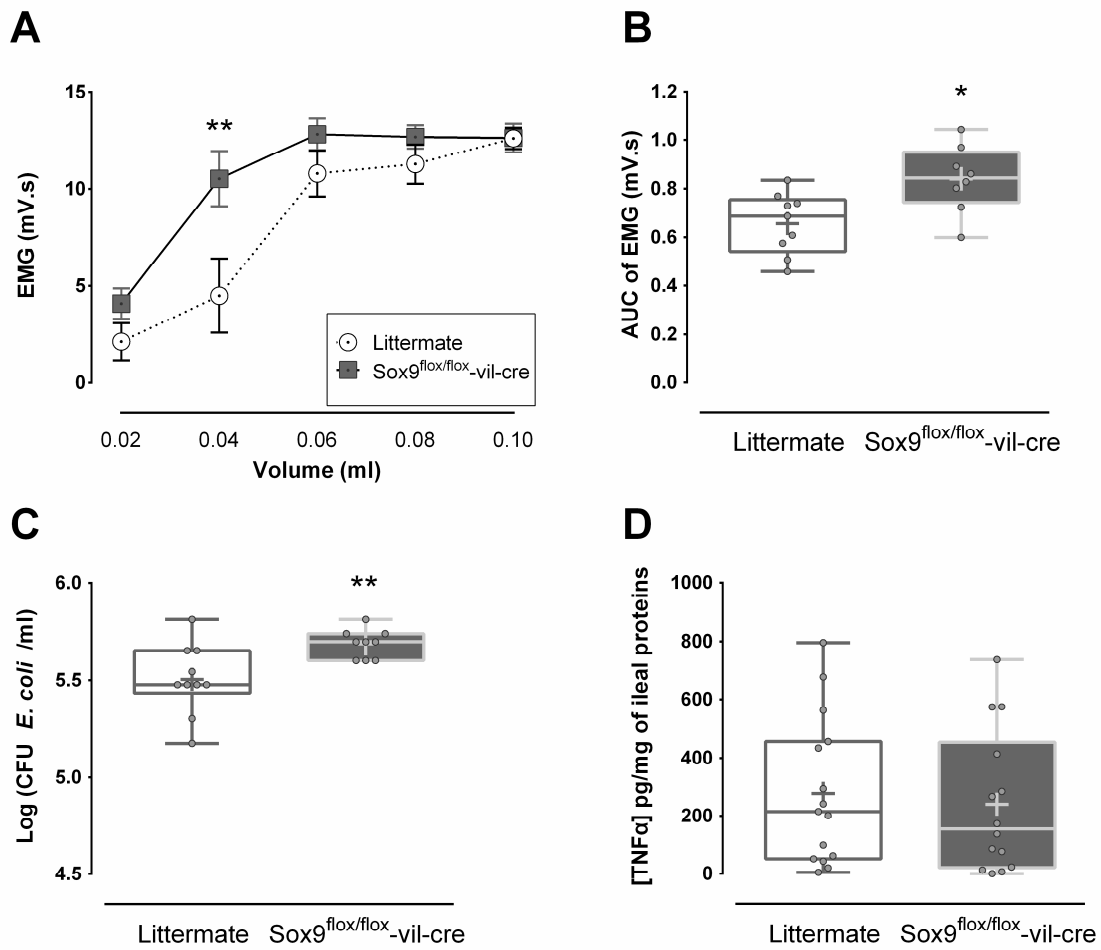
Figure 2



Comment citer ce document :

Riba, A., Olier, M., Lacroix Lamandé, S., Lencina, C., Bacquié, V., Harkat, C., Gillet, M., Baron, M., Sommer, C., Mallet, V., Salvador Cartier, C., Laurent, F., Théodorou, V., Ménard, S. (2017). Paneth cell defects induce microbiota dysbiosis in mice and promote visceral hypersensitivity. *Gastroenterology*. 153 (6). 1594-1606. DOI : 10.1053/j.gastro.2017.08.044

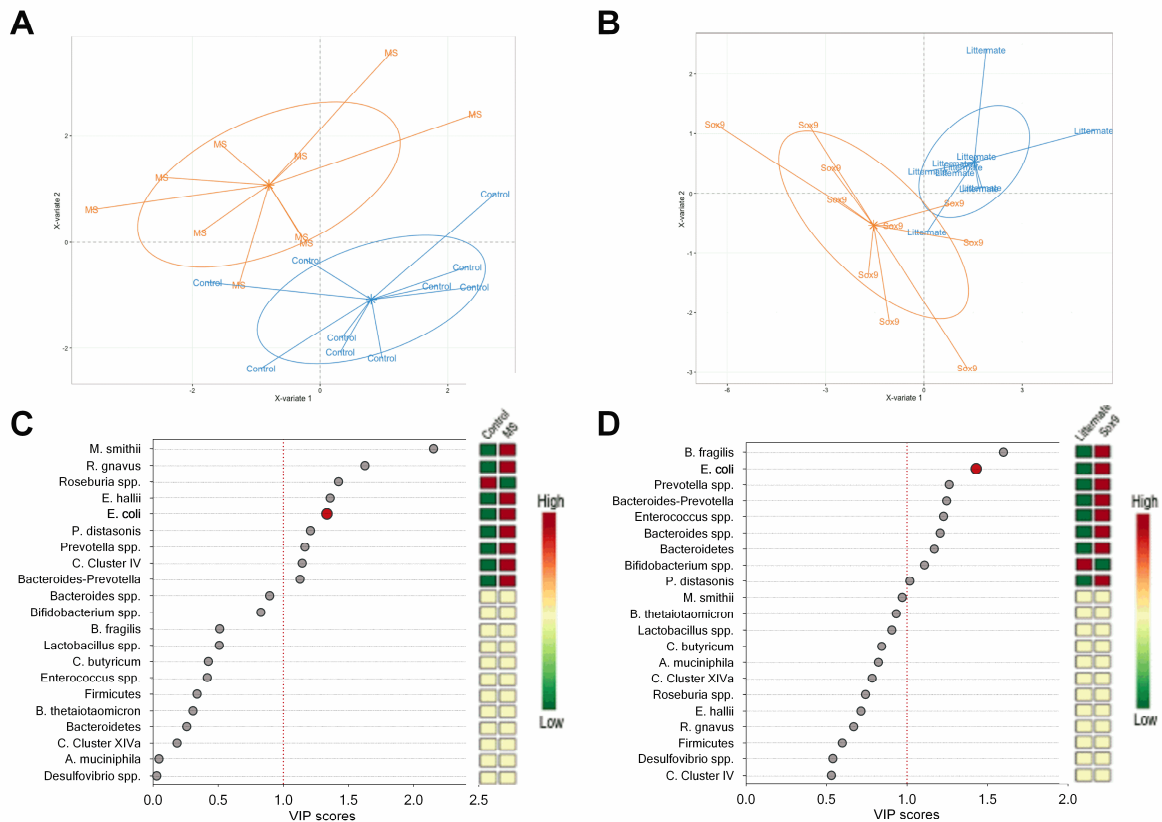
Figure 3



Comment citer ce document :

Riba, A., Olier, M., Lacroix Lamandé, S., Lencina, C., Bacquié, V., Harkat, C., Gillet, M., Baron, M., Sommer, C., Mallet, V., Salvador Cartier, C., Laurent, F., Théodorou, V., Ménard, S. (2017). Paneth cell defects induce microbiota dysbiosis in mice and promote visceral hypersensitivity. *Gastroenterology*. 153 (6), 1594-1606. DOI : 10.1053/j.gastro.2017.08.044

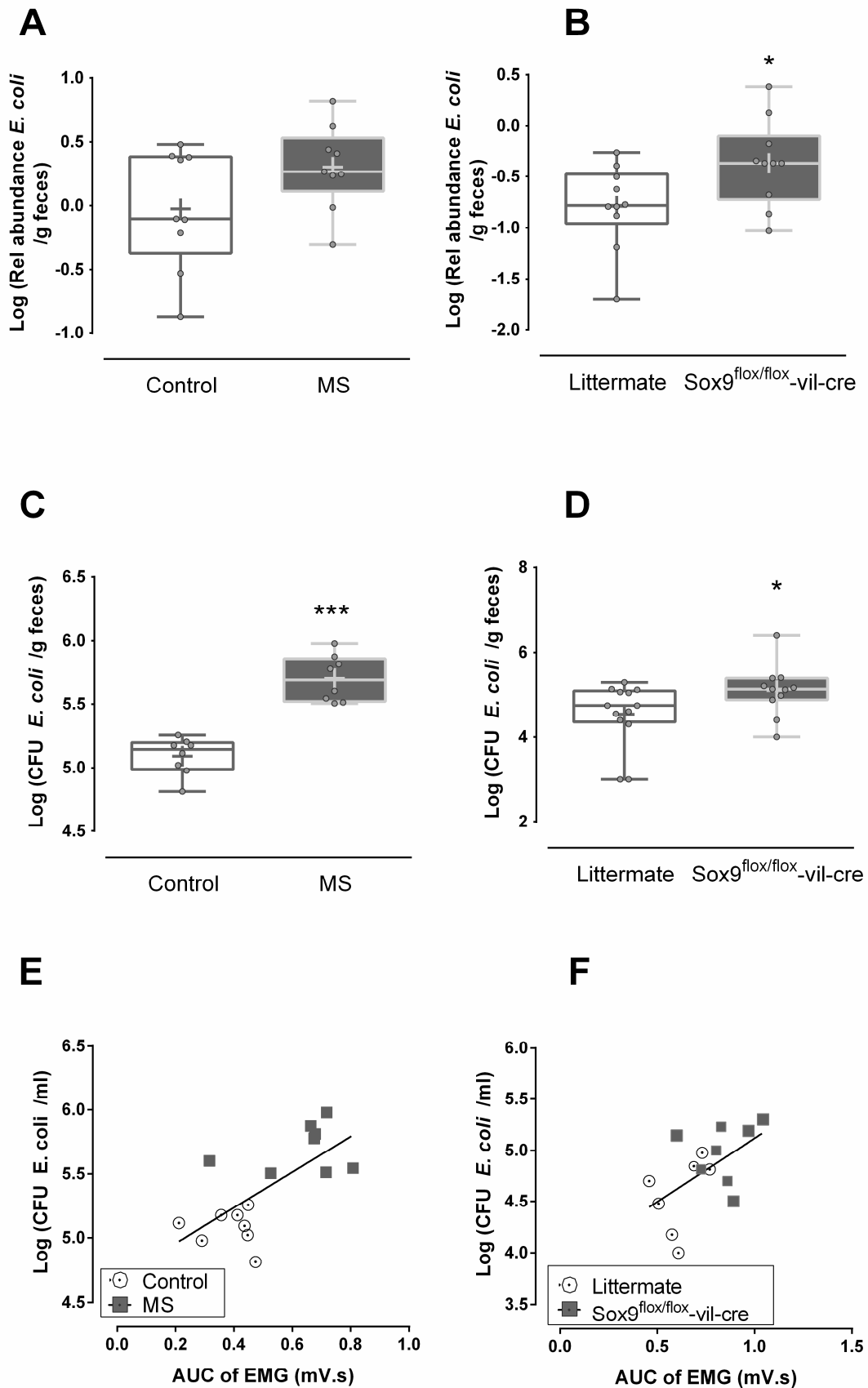
Figure 4



Comment citer ce document :

Riba, A., Olier, M., Lacroix Lamandé, S., Lencina, C., Bacquié, V., Harkat, C., Gillet, M., Baron, M., Sommer, C., Mallet, V., Salvador Cartier, C., Laurent, F., Théodorou, V., Ménard, S. (2017). Paneth cell defects induce microbiota dysbiosis in mice and promote visceral hypersensitivity. *Gastroenterology*. 153 (6). 1594-1606. DOI : 10.1053/j.gastro.2017.08.044

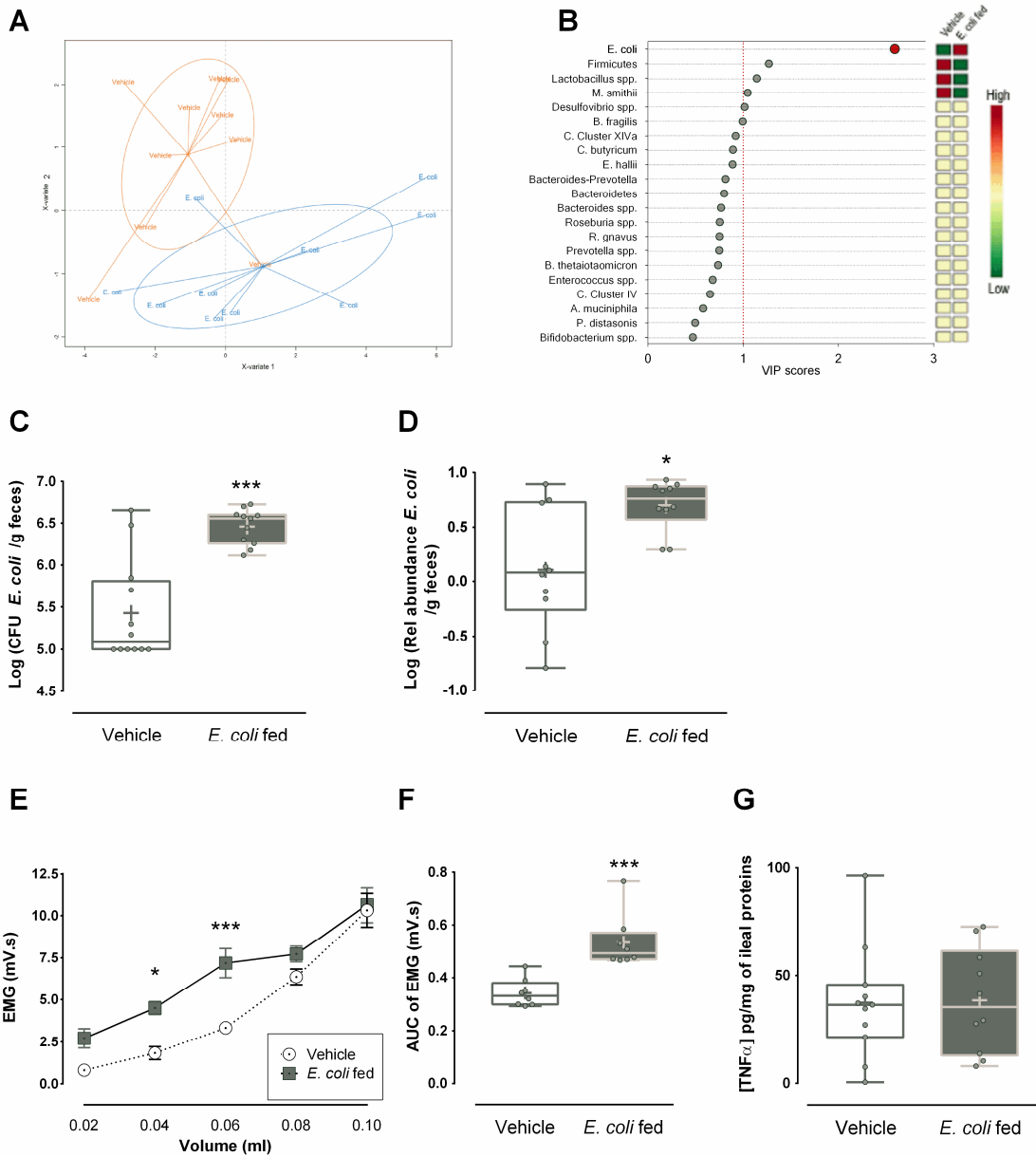
Figure 5



Comment citer ce document :

Riba, A., Olier, M., Lacroix Lamandé, S., Lencina, C., Bacquié, V., Harkat, C., Gillet, M., Baron, M., Sommer, C., Mallet, V., Salvador Cartier, C., Laurent, F., Théodorou, V., Ménard, S. (2017). Paneth cell defects induce microbiota dysbiosis in mice and promote visceral hypersensitivity. *Gastroenterology*. 153 (6). 1594-1606. DOI : 10.1053/j.gastro.2017.08.044

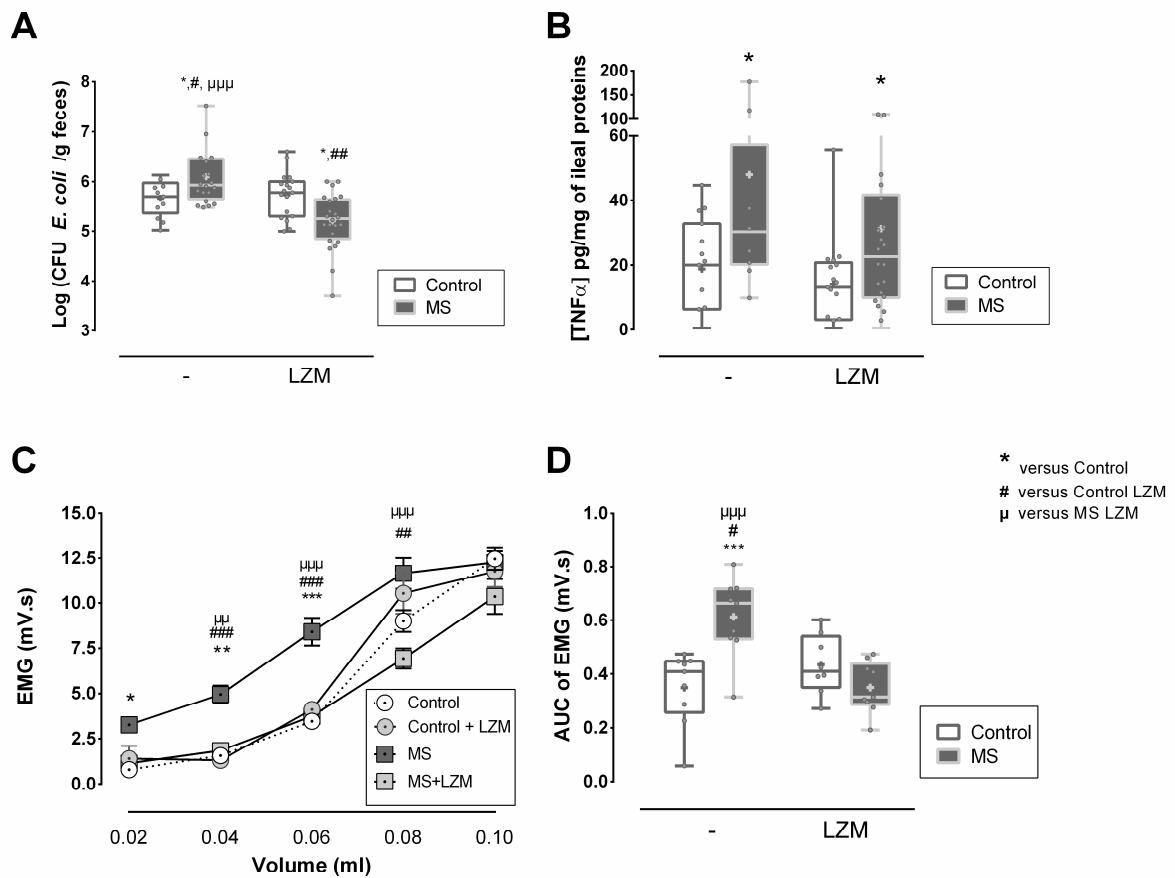
Figure 6



Comment citer ce document :

Riba, A., Olier, M., Lacroix Lamandé, S., Lencina, C., Bacquié, V., Harkat, C., Gillet, M., Baron, M., Sommer, C., Mallet, V., Salvador Cartier, C., Laurent, F., Théodorou, V., Ménard, S. (2017). Paneth cell defects induce microbiota dysbiosis in mice and promote visceral hypersensitivity. *Gastroenterology*. 153 (6). 1594-1606. DOI : 10.1053/j.gastro.2017.08.044

Figure 7



Comment citer ce document :

Riba, A., Olier, M., Lacroix Lamandé, S., Lencina, C., Bacquié, V., Harkat, C., Gillet, M., Baron, M., Sommer, C., Mallet, V., Salvador Cartier, C., Laurent, F., Théodorou, V., Ménard, S. (2017). Paneth cell defects induce microbiota dysbiosis in mice and promote visceral hypersensitivity. *Gastroenterology*. 153 (6). 1594-1606. DOI : 10.1053/j.gastro.2017.08.044

Supplementary Materials and Methods

Mouse models

In all experiments, mice were kept at a constant temperature (22+/-1°C) and maintained on a 12:12h light/dark cycle (light on at 7h30 am). Food (Harlan, Gannat, France) and water were available *ad libitum*. After delivery (D1), litters were homogenized to 6±1 pups. Weaning was performed on D21, siblings were sex matched.

Maternal Separation protocol

Nulliparous female C3H/HeN mice (Janvier, Roubaix, France) were mated with male for 4 days. Maternal separation (MS) was performed daily for three consecutive hours (from 9 am to 12 pm). Pups were kept in controlled temperature (27+/-1°C). MS was repeated for 10 working days, weekend excluded, between D2 and D15. Control pups were left with their dam. From D15 to D21, all pups were maintained with their dam.

Oral gavage of commensal E. coli streptomycin resistant

Live *E. coli* were isolated from feces of naïve healthy C3H/HeN mice by culture on selective ChromID coli plates (Biomérieux, Marcy L'étoile, France). Grown colonies belonged to B1 phylogenetic group. Further characterization of one representative isolate revealed to belong to the O18 serogroup and none of checked virulence genes was harbored (*lt*, *sTa*, *sTb*, *stx1*, *stx2*, *eae*, *hly*, *cnf*, *Afa*, *cdt*, *pks*). In order to facilitate monitoring of this commensal *E. coli* isolate in feces of mice after gavage, a spontaneous streptomycin resistant mutant of the commensal isolate was generated by plating a PBS-washed overnight culture on LB 1% agar plates supplemented with 50µg/ml streptomycin. Growing colonies were then subcultured either on LB 1% agar plate alone, LB 1% agar supplemented with 50µg/ml or 500µg/ml streptomycin in parallel. Colony able to growth on all three conditions was selected and frozen at -80°C until use for gavage.

IL17, IL22 and IL10 measurement in the ileum

IL17, IL22 and IL10 were measured in supernatant of ileal fragments previously treated as follow. Frozen ileal fragments were suspended in RIPA buffer (0.5% deoxycholate, 0.1% SDS and 1% Igepal in TBS) containing complete anti protease cocktail (Roche), protein concentrations were measured using BCA uptima kit (Interchim).

IL17, IL22 and IL10 present in ileal tissues were assayed using commercial enzyme linked immunosorbent assays (ELISA kits; Duoset R&D Systems, Lille, France). Cytokines concentrations were normalized per mg of proteins in the supernatant and results expressed in pg of cytokine per mg of proteins.

Lysozyme expression in Paneth cells

Ileal samples were fixed in 4% formal, dehydrated through graded ethanol and embedded in paraffin. Sections (5µm) were rehydrated and submerged in antigen retrieval solution (citrate buffer, 10mM, pH6, 99°C) for 30 minutes. After incubation in blocking solution (PBS 0,01% Tween 20, 1% bovine serum albumin and 2% donkey normal serum) for 15 min, sections were incubated with rabbit anti-mouse lysozyme antibody (1/100, overnight, +4°C ;Abcam, Paris, France) followed by a Alexa fluor 488-conjugated donkey anti-rabbit IgG (0.75µg/ml, 1H, Room temperature, Jackson, Suffolk). Antibody used would stained the mouse M and P lysozyme isoforms. Sections were incubated with Alexa fluor 594-conjugated Wheat Germ Agglutinin (WGA, 10µg/ml, 45 min; Invitrogen, Life Technology, Cergy Pontoise, France), mounted in Prolong gold antifade mounting medium with DAPI (Invitrogen) and examined under a Nikon 90i fluorescence microscope. Lysozyme fluorescence intensity in Paneth cells were quantified employing the software Nis-Elements Ar (Nikon, Champigny sur Marne, France) and results were expressed in fluorescence intensity per cell. Analyses were done on five well preserved crypts per animal and on five animals from each group.

Lysozyme activity in fecal content

Fecal proteins were mechanically extracted after rehydration of frozen feces in 500µl of PBS (10mM; pH7.2). After 10 minutes of centrifugation at 1600g, supernatants were sterilized with a 0.22 µm filter and frozen (-80°C). Fecal protein concentration was measured using BCA protein Assay kit, Uptima (Interchim, Montluçon, France). Activity of lysozyme against the peptidoglycan was determined using the EnzChek® Lysozyme Assay Kit (Molecular probes, life technology, St Aubin, France).

Fecal microbiota composition

Changes in the relative abundance of 21 relevant microbial 16S rRNA gene targets (Supplementary table 1) was obtained using the GULDA platform approach (Bergström *et al*, 2012b, 2012a) with minor adaptations (Yvon *et al*, 2016). According to this method, the universal bacterial primer set (All phyla) was included as the reference gene (four technical replicas of each amplification). Each 384-well PCR plate (MicroAmp optical reaction plates, Applied Biosystems, Naerum, Denmark) accommodated simultaneous analysis of 8 DNA samples per group. Quantitative real-time PCR was performed in duplicate on an ViiA7 from Applied Biosystems in a total volume of 5 µl containing 2,5 µl 2x Power SYBR Green PCR Master Mix (Applied biosystems), 0,18 µl of each primer (10 µM), 1 µl template DNA, and 1,14 µl nuclease-free water. Liquid handling was performed with a Bravo platform (Agilent Technologies, Santa Clara, USA). Following the previously described thermocycling program, the raw fluorescence data recorded by the ViiA7 RUO Software were exported to the LinRegPCR program to perform baseline correction, calculate the mean PCR efficiency per amplicon group and calculate the initial quantities No (arbitrary fluorescence units) for each amplicon. The relative abundance of the 21 specific amplicon groups were obtained by normalization to the No value obtained for the universal bacterial amplicon group determined

in the same array (No, specific/No, universal). A limit of detection of 10^{-6} (No, specific/No, universal) was set and samples below this limit were set to $5 \cdot 10^{-6}$.

REFERENCES

- Bergström A, Kristensen MB, Bahl MI, Metzdorff SB, Fink LN, Frøkiær H & Licht TR Nature of bacterial colonization influences transcription of mucin genes in mice during the first week of life. *BMC Res. Notes* (2012a) **5**: 402
- Bergström A, Licht TR, Wilcks A, Andersen JB, Schmidt LR, Grønlund HA, Vignæs LK, Michaelsen KF & Bahl MI Introducing GUt Low-Density Array (GULDA) - a validated approach for qPCR-based intestinal microbial community analysis. *FEMS Microbiol. Lett.* (2012b) **337**: 38–47
- Yvon S, Olier M, Leveque M, Jard G, Tormo H, Haimoud-Lekhal DA, Peter M & Eutamène H Donkey milk consumption exerts anti-inflammatory properties by normalizing antimicrobial peptides levels in Paneth's cells in a model of ileitis in mice. *Eur. J. Nutr.* (2016) Available at: <http://link.springer.com/10.1007/s00394-016-1304-z>

Supplementary Table 1

Supplementary Table 1. Primers used in this study

Phylum	Class/Family/ Genus	Species /Group	Primers sequences (5'-3')
All phyla	All	All	ACTCCTACGGGAGGAGCAGT GTATTACCGGGCTGCTGGCAC
Actinobacteria	<i>Bifidobacterium</i>	<i>spp.</i>	CGCGTCYGGTGTAAAG CCCCACATCCAGCATCCA
Bacteroidetes	All	All	GGARCATGTGGTTTAATTCGATGAT AGCTGACGACAAACCATGCAG
Bacteroidetes	<i>Bacteroides /Prevotella</i>	<i>spp.</i>	GAGAGGAAGTCCCCAC CGCTACTGGCTGTTTCCAG
Bacteroidetes	<i>Bacteroides</i>	<i>spp.</i>	CGATGGATAGGGTCTGAGAGGA GCTGGCACGGAGTTAGCCGA
Bacteroidetes	<i>Bacteroides</i>	<i>fragilis group</i>	CTGAACCAGCCAAGTAGCG CGCAAACTTCACTCACTGACTTA
Bacteroidetes	<i>Bacteroides</i>	<i>thetaiotaomicron</i>	GGCAGCATTTCAGTTGCTTG GGTACATACAAAATCCACACGT
Bacteroidetes	<i>Parabacteroides</i>	<i>distasonis</i> [†]	TGATCCCTTGTGCTGCT ATCCCTCATTCGGA
Bacteroidetes	<i>Prevotella</i>	<i>spp.</i>	CACCAAGGCGACGATCA GGATAACGCCYGGACCT
Firmicutes	All	All	TGAAACTYAAAGGAATTGACG ACCATGCACACCTGTC
Firmicutes	<i>Lactobacillus</i>	<i>spp.</i>	AGCAGTAGGGAATCTTCCA CACCGCTACACATGGAG
Firmicutes	<i>Clostridium</i>	<i>butyricum</i> (Cluster I)	GTGCCGCCGCTAACGCATTAAGTAT ACCATGCACACCTGTCTTCTGCC
Firmicutes	<i>Clostridia</i>	Cluster IV (<i>C. leptum</i> group)	GCACAAGCAGTGGAGT CTTCTCCGTTTTGTCAA
Firmicutes	<i>Clostridia</i>	Cluster XIVa (<i>C. coccoides</i> - <i>E. rectale</i> group)	ACTCCTACGGGAGGACG GCTTCTTAGTCAGGTACCGTCAT
Firmicutes	<i>Clostridia/Lachnospiraceae</i>	<i>Ruminococcus gnavus</i> (<i>Blautia</i>)	GGACTGCATTTGGAAGTGTGAG AACGTGAGTATCGTCCAGAAAG
Firmicutes	<i>Eubacterium</i>	<i>hallii</i>	GCCTAGTGGCAGTGCAA GCACCGRAGCCTATACGG
Firmicutes	<i>Roseburia</i>	<i>spp.</i>	TACTGCATTGAAACTGTGCG CGGCACGAAGAGCAAT
Firmicutes	<i>Enterococcus</i>	<i>spp.</i>	CCCTTATTGTTAGTGCATCATT ACTCGTTGTACTTCCATTGT
Proteobacteria	<i>Escherichia</i>	<i>coli</i>	CATGCCGGTGTATGAAGAA CGGGTAACGTAATGAGCAAA
Proteobacteria	<i>Desulfovibrio</i>	<i>spp.</i>	CCGTAGATATCTGGAGGAACATCAG ACATCTAGCATCCATGTTTACAGC
Verrucomicrobia	<i>Akkermansia</i>	<i>muciniphila</i>	CAGCACGTGAAGGTGGGGAC CCTTGCAGTTGGCTTCCAGAT
Euryarchaeota	<i>Methanobrevibacter</i>	<i>smithii</i>	CCGGGTACTAATCCGGTTC CTCCAGGGTAGAGGTGAAA

[†]Primer set *B. distasonis* targets the 16S–23S rRNA gene intergenic spacer region.

Comment citer ce document :

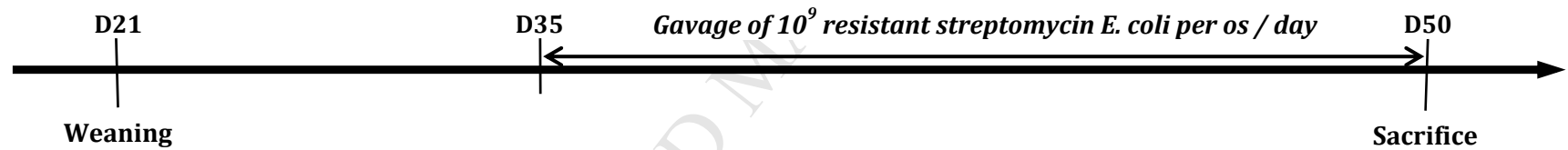
Riba, A., Olier, M., Lacroix Lamandé, S., Lencina, C., Bacquié, V., Harkat, C., Gillet, M., Baron, M., Sommer, C., Mallet, V., Salvador Cartier, C., Laurent, F., Théodorou, V., Ménard, S. (2017). Paneth cell defects induce microbiota dysbiosis in mice and promote visceral hypersensitivity. *Gastroenterology*, 153 (6), 1594-1606. DOI : 10.1053/j.gastro.2017.08.044

Supplementary Figure 1

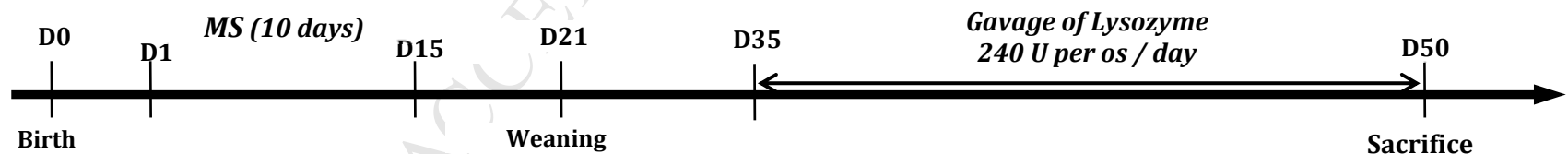
A



B



C

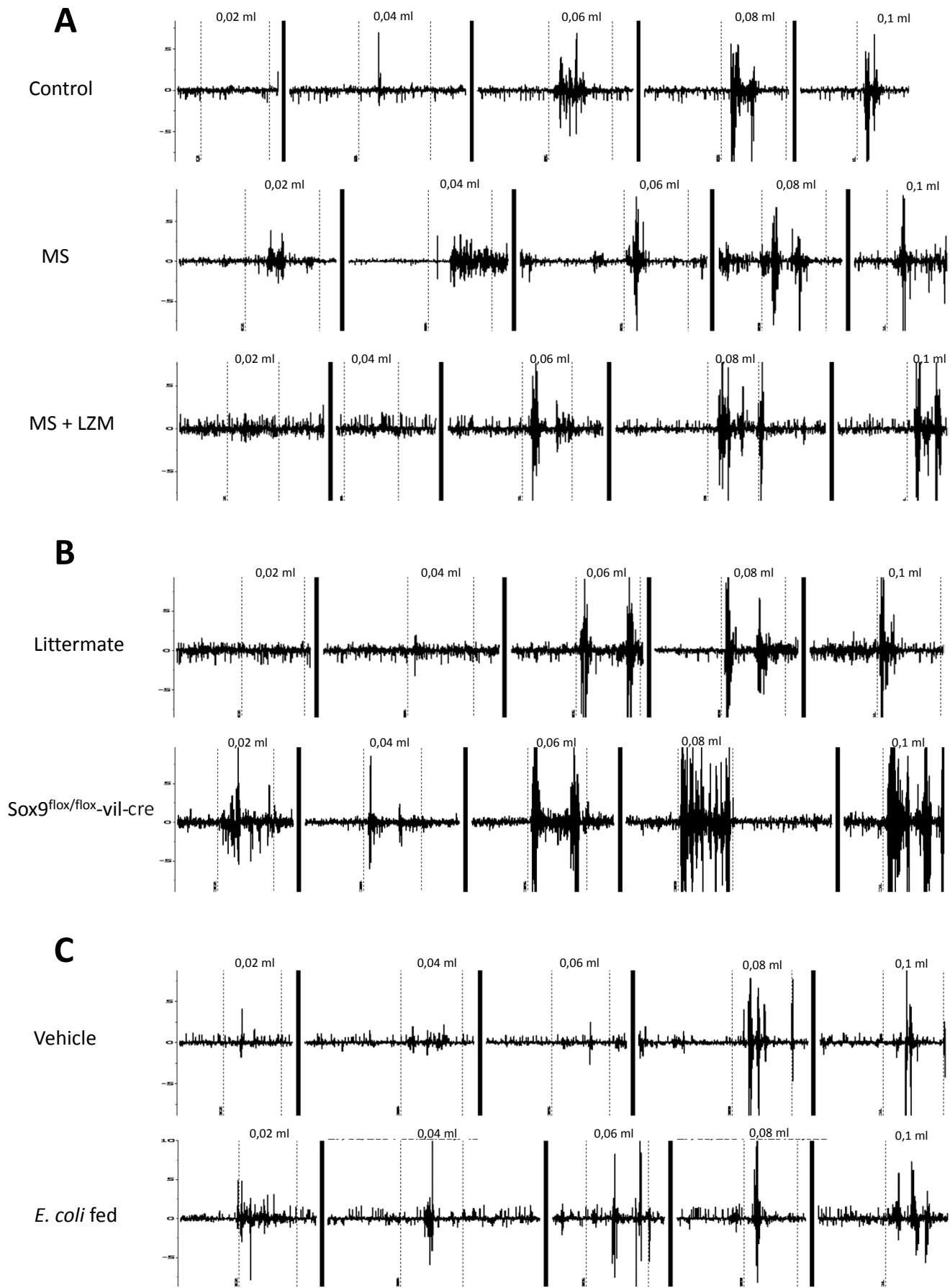


Supplementary Figure 1- Experimental protocols. Experimental protocol of Maternal Separation (MS) (A). Experimental protocol of *E. coli* gavage (B). Experimental protocol of lysozyme gavage (C)

Comment citer ce document :

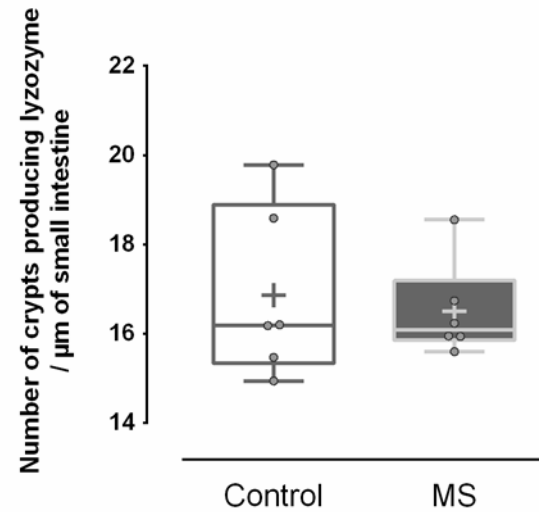
Riba, A., Olier, M., Lacroix Lamandé, S., Lencina, C., Bacquié, V., Harkat, C., Gillet, M., Baron, M., Sommer, C., Mallet, V., Salvador Cartier, C., Laurent, F., Théodorou, V., Ménard, S. (2017). Paneth cell defects induce microbiota dysbiosis in mice and promote visceral hypersensitivity. *Gastroenterology*, 153 (6), 1594-1606. DOI : 10.1053/j.gastro.2017.08.044

Supplementary Figure 2



Supplementary Figure 2- Representative, illustrative EMG recording of one mice per group: control, MS mice of MS mice receiving oral gavage of LZM (A) littermate and Sox9^{flox/flox}-vil-cre (B) and vehicle or mice receiving *E. coli* by oral gavage (C).

Supplementary Figure 3

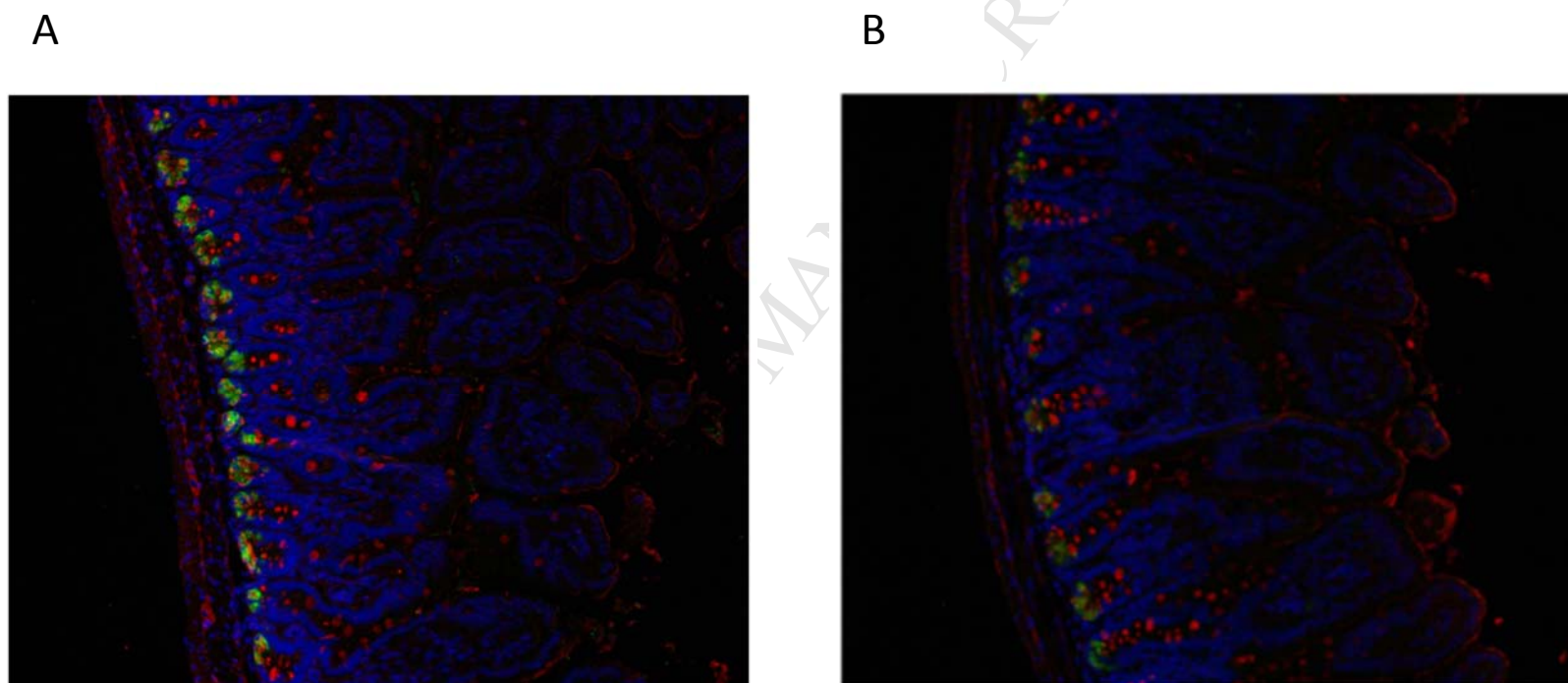


Supplementary Figure 3- Number of crypts stained with lysozyme in small intestine on MS mice (n=6 per group)

Comment citer ce document :

Riba, A., Olier, M., Lacroix Lamandé, S., Lencina, C., Bacquié, V., Harkat, C., Gillet, M., Baron, M., Sommer, C., Mallet, V., Salvador Cartier, C., Laurent, F., Théodorou, V., Ménard, S. (2017). Paneth cell defects induce microbiota dysbiosis in mice and promote visceral hypersensitivity. *Gastroenterology*, 153 (6), 1594-1606. DOI : 10.1053/j.gastro.2017.08.044

Supplementary Figure 4

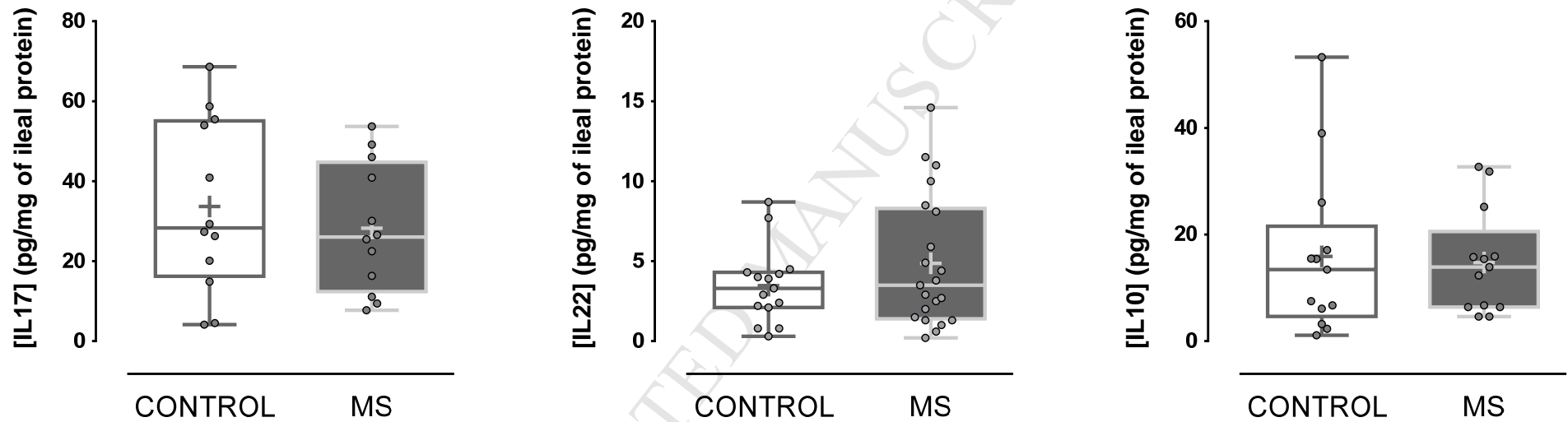


Supplementary Figure 4- Immunostaining of ileum paraffin section with anti-lysozyme-(FITC) (Green) Wheat germ agglutinin-(Texas red) (red) and DAPI (blue) (10 fold magnification) in control mice (A) and maternally separated mice (B) (n=5-6 per group)

Comment citer ce document :

Riba, A., Olier, M., Lacroix Lamandé, S., Lencina, C., Bacquié, V., Harkat, C., Gillet, M., Baron, M., Sommer, C., Mallet, V., Salvador Cartier, C., Laurent, F., Théodorou, V., Ménard, S. (2017). Paneth cell defects induce microbiota dysbiosis in mice and promote visceral hypersensitivity. *Gastroenterology*, 153 (6), 1594-1606. DOI : 10.1053/j.gastro.2017.08.044

Supplementary Figure 5

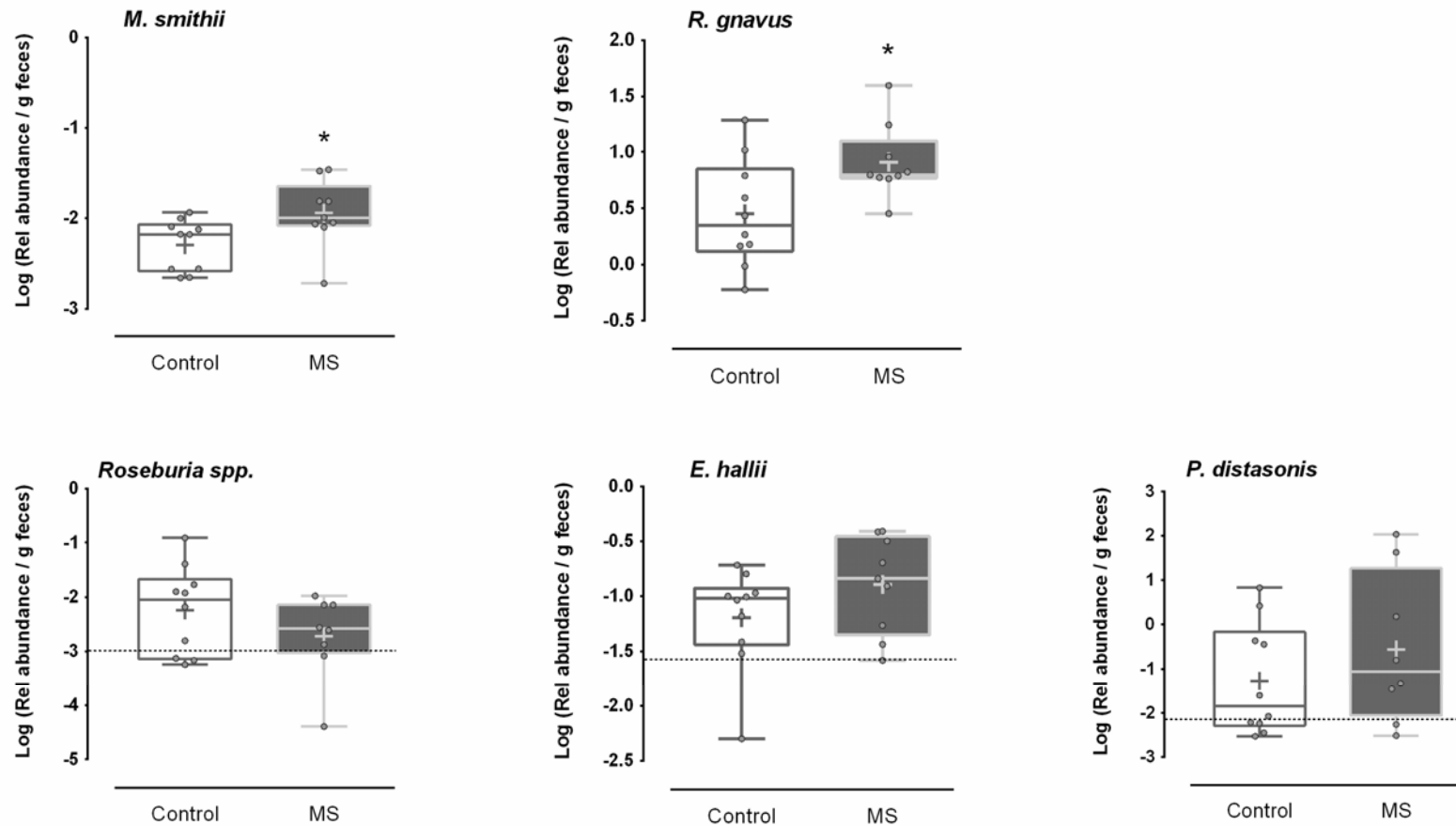


Supplementary Figure 5- Ileal concentration of IL17, IL22 and IL10 measured by ELISA (n=12-21 per group)

Comment citer ce document :

Riba, A., Olier, M., Lacroix Lamandé, S., Lencina, C., Bacquié, V., Harkat, C., Gillet, M., Baron, M., Sommer, C., Mallet, V., Salvador Cartier, C., Laurent, F., Théodorou, V., Ménard, S. (2017). Paneth cell defects induce microbiota dysbiosis in mice and promote visceral hypersensitivity. *Gastroenterology*, 153 (6), 1594-1606. DOI : 10.1053/j.gastro.2017.08.044

Supplementary Figure 6

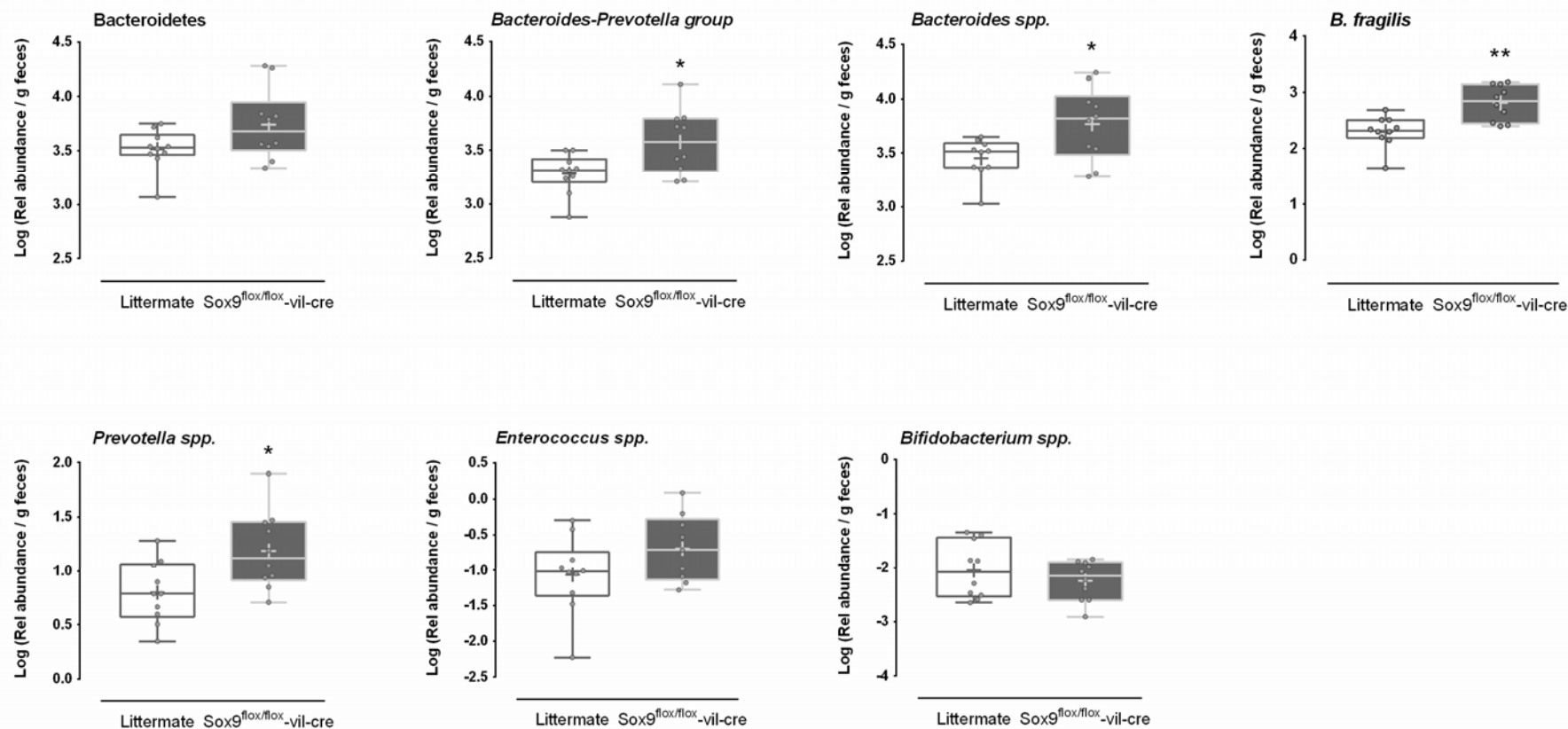


Supplementary Figure 6- Relative abundances of fecal microbial communities identified as important contributors in addition to these of *E. coli* to differences between MS mice and control (n=9 to 10 mice per group). *: $p < 0.05$ with control.

Comment citer ce document :

Riba, A., Olier, M., Lacroix Lamandé, S., Lencina, C., Bacquié, V., Harkat, C., Gillet, M., Baron, M., Sommer, C., Mallet, V., Salvador Cartier, C., Laurent, F., Théodorou, V., Ménard, S. (2017). Paneth cell defects induce microbiota dysbiosis in mice and promote visceral hypersensitivity. *Gastroenterology*, 153 (6), 1594-1606. DOI : 10.1053/j.gastro.2017.08.044

Supplementary Figure 7

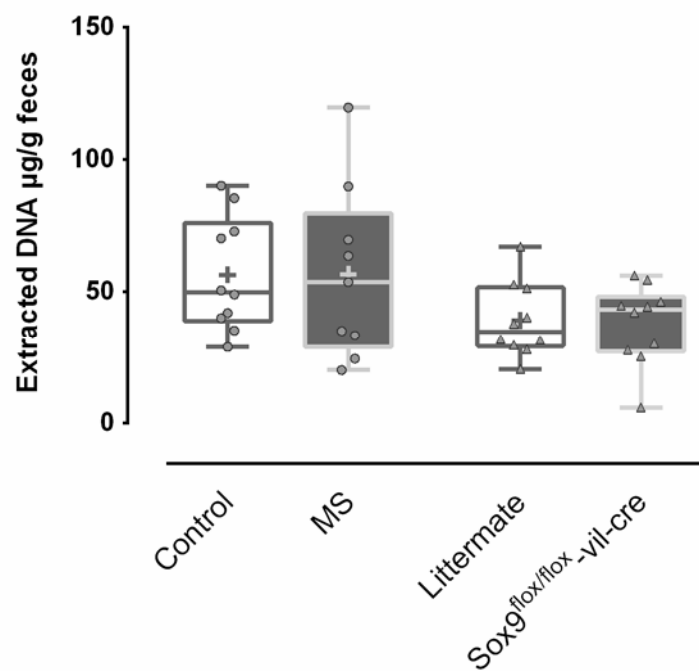


Supplementary Figure 7 - Relative abundances of fecal microbial communities identified as important contributors in addition to these of *E. coli* to differences between Sox9^{flox/flox}-vil-cre mice and littermate (n=9 to 10 mice per group). *: $p < 0.05$ with littermate.

Comment citer ce document :

Riba, A., Olier, M., Lacroix Lamandé, S., Lencina, C., Bacquié, V., Harkat, C., Gillet, M., Baron, M., Sommer, C., Mallet, V., Salvador Cartier, C., Laurent, F., Théodorou, V., Ménard, S. (2017). Paneth cell defects induce microbiota dysbiosis in mice and promote visceral hypersensitivity. *Gastroenterology*, 153 (6), 1594-1606. DOI : 10.1053/j.gastro.2017.08.044

Supplementary Figure 8



Supplementary Figure 8 – Microbial genomic DNA extracted per gram feces (n=9 to 10 mice per group).

Comment citer ce document :

Riba, A., Olier, M., Lacroix Lamandé, S., Lencina, C., Bacquié, V., Harkat, C., Gillet, M., Baron, M., Sommer, C., Mallet, V., Salvador Cartier, C., Laurent, F., Théodorou, V., Ménard, S. (2017). Paneth cell defects induce microbiota dysbiosis in mice and promote visceral hypersensitivity. *Gastroenterology*, 153 (6), 1594-1606. DOI : 10.1053/j.gastro.2017.08.044